NI

NASA Technical Memorandum 83193

(NASA-TM-83193) THE EFFECTS OF LATERAL AERODYNAMIC UNCERTAINTIES ON THE HANDLING QUALITIES OF THE SPACE SHUTTLE ORBITER AT MACH NUMBERS OF 1.5 AND .6 (NASA) 42 p HC A03/MF A01 CSCL 01C G3/05

N82-11051

Unclas 08177

THE EFFECTS OF LATERAL AERODYNAMIC UNCERTAINTIES ON THE HANDLING QUALITIES OF THE SPACE SHUTTLE ORBITER AT MACH NUMBERS OF 1.5 AND .6

Lawrence W. Brown

September 1981

National Aeronautics and Space Administration

Langley Research Center
Hampton Virginia 23665

THE EFFECTS OF LATERAL AERODYNAMIC UNCERTAINTIES ON THE HANDLING QUALITIES OF THE SPACE SHUTTLE ORBITER AT MACH NUMBERS OF 1.5 AND .6

Lawrence W. Brown

SUMMARY

The effects of aerodynamic uncertainties on the handling qualities of the space shuttle orbiter were investigated with the use of six-degree-of-freedom, nonlinear equations of motion on the hybrid computer system. Flight condition characteristics for Mach numbers of 1.5 and .6 for the nominal and off nominal angle of attack conditions were selected for this investigation. Results revealed that at the low Mach number condition (M = .6) only a few problems existed for the angle of attack range and the many combinations of large aerodynamic variations considered. Moreover, none of these problems were considered to be related to poor handling qualities. For the angle of attack conditions considered at the high Mach number (M = 1.5), problems existed with reduction of roll rate which can result in roll reversal conditions. In many cases, sideslip became proverse and increased rudder deflections and yaw jets were required.

INTRODUCTION

Flight simulations are necessary in the planning and directing of flight test programs for experimental and research-type aircraft. An accurate simulation of the aircraft's motion response to control inputs necessitates a complete compilation of the characteristics of the aerodynamic derivatives which are indicative of the actual aircraft. In predicting the aerodynamic derivatives from wind tunnel results, the accuracy of the prediction is dependent upon the Reynolds number difference between test conditions and flight; the manufacturing difference between the model and actual configuration; aft nominal conditions such as variation in angle of attack and altitude; and other anamolies. It is important that the prediction of the aerodynamic derivatives of the space shuttle orbiter be even more accurate than most vehicles tested since this unpowered aircraft will not have engines to modulate the flight conditions.

In the piloted simulation of the space shuttle orbiter for nominal flight conditions, satisfactory flying qualities have been predicted. However, differences in the aerodynamic derivatives due to the reasons above could cause significant discrepancies in the prediction of the orbiter responses. These discrepancies could require a placard on the center-of-gravity position operational range, lead to control system rate limiting; cause excessive fuel usage in the reaction control system (RCS); cause excessive pilot workload; and possibly cause loss of aircraft.

In recognition of these conditions, an investigation was undertaken on a hybrid computer to determine the effects these aerodynamic uncertainties would have on the handling qualities of the space shuttle orbiter. A large number of variations in the aerodynamic derivatives were applied to the nominal and off nominal flight conditions at Mach numbers of 1.5 and .6.

SYMBOLS

The aerodynamic parameters are referenced to a system of body axes with the origin at the vehicle center-of-gravity (Fig. 1). The positive sense of the angles, forces, moments, and angular velocities are also shown.

A_y	lateral acceleration, g's
b	wing span, m (ft)
$\bar{c}$	wing mean aerodynamic chord, m (ft)
C_l	rolling moment coefficient, Mx/gsb
C_n	yawing moment coefficient, Mz/gsb
C_y	side/force coefficient, Fy/gs
F_x, F_y, F_z	aerodynamic forces along the x, y, z body axes, n (lb)
g	acceleration due to gravity, m/sec^2 (ft/sec^2)
h	altitude, m (ft)
I_x, I_y, I_z	moments of inertia about the aircraft body axes, $kg - m^2$ ($slug - ft^2$)
I_{xz}	product of inertia about the aircraft body axes, $kg - m^2$ ($slug - ft^2$)
KP1,KP2,KP3,KR1 KR2,KR3,KNY,KJ1	lateral control system gains
M	Mach number
M_x, M_y, M_z	aerodynamic moments about the x, y, z body axes, m - n (ft - lb)
m	aircraft mass, kg (slugs)
p	roll rate about the body x axis, rad/sec

p_c	roll rate command, rad/sec
PR	aileron - rudder interconnect
q	pitch rate about the body y axis, rad/sec
$\bar{q}$	dynamic pressure, N/m^2 (lb/ft^2)
q_m	maximum dynamic pressure, N/m^2 (lb/ft^2)
r	yaw rate about the z body axis, rad/sec
r'	stability axis yaw rate, $r - \frac{g}{V} \cos \theta \sin \phi$
S	wing area, m^2 (ft^2)
t	time, sec
UZC	commanded yaw jets, m/sec^2 (ft/sec^2)
V	velocity, m/sec (ft/sec)
x,y,z	airplane body axes, origin at center-of-gravity
α	angle of attack, deg
α_t	trim angle of attack, deg
β	angle of sideslip, deg
ϕ	angle of roll, deg
θ	angle of pitch, deg
δ_a	roll control input $\delta_a = (\delta_{e_l} - \delta_{e_r})/2$, positive in direction to cause positive roll rate, deg
δ_{a_c}	commanded roll control input, deg
δ_r	rudder deflection, positive deflection cause left yawing moments, deg
δ_{r_c}	commanded rudder deflection, deg
δ_{e_l}	left elevon deflection, positive for trailing edge down, deg
δ_{e_r}	right elevon deflection, positive for trailing edge down, deg

$$C_{l_\beta} = \frac{\partial C_l}{\partial_\beta} \qquad C_{n_\beta} = \frac{\partial C_n}{\partial_\beta} \qquad C_{y_\beta} = \frac{\partial C_y}{\partial_\beta}$$

$$C_{l_p} = \frac{\partial C_l}{\partial\left(\frac{Pb}{2r}\right)} \qquad C_{n_p} = \frac{\partial C_n}{\partial(pb/2v)} \qquad C_{y_{\delta a}} = \frac{\partial C_y}{\partial \delta a}$$

$$C_{l_r} = \frac{\partial C_l}{\partial(rb/sv)} \qquad C_{n_r} = \frac{\partial C_n}{\partial(rb/2v)} \qquad C_{y_{\delta r}} = \frac{\partial C_y}{\partial \delta r}$$

$$C_{l_{\delta a}} = \frac{\partial C_l}{\partial \delta a} \qquad C_{n_{\delta a}} = \frac{\partial C_n}{\partial \delta a}$$

$$C_{l_{\delta r}} = \frac{\partial C_l}{\partial \delta r} \qquad C_{n_{\delta r}} = \frac{\partial C_n}{\partial \delta r}$$

DESCRIPTION OF VEHICLE

Physical and Control Characteristics

The space shuttle orbiter (Fig. 2) consists of a fuselage of 33.77 m (107.53 ft) in length with a 45^0 swept wing and a vertical tail. The mass and physical characteristics are presented in table 1. The orbiter is a reusable space vehicle which flies back from near-earth orbit along a prescribed trajectory (Fig. 3) for an unpowered landing at a designated airfield.

The orbiter uses a combination of spacecraft and aircraft control effectors. At low dynamic pressures it is controlled using reaction control thrusters (like a spacecraft). As dynamic pressure builds up, there is a gradual transition from using thrusters for control to using the large aerodynamic surfaces.

The primary control surfaces are the elevons--deflected symmetrically for pitch control and differentially for roll control--and conventional rudder for yaw control. The rudder is split to provide a speed brake for improved directional stability (C_{n_β}) at hypersonic/supersonic speeds and energy management (by modulating lift/drag ratio) in the subsonic region. The body flap is added to supplement the elevons for pitch control. The control surface limits are presented in table 1.

Lateral Control System

In this study only Mach numbers of 1.5 and lower were considered for which the lateral control system is described in figure 4. In the roll control channel, as depicted in the block diagram, the pilot's input from a center stick is converted to a roll rate command and summed with the stability axis roll rate to create an aileron command. The aileron surface deflection is limited to $\pm 10^{\circ}$. The roll control signal is also fed to the rudder channel by an aileron - rudder interconnect.

In the rudder control channel the lateral acceleration is filtered and combined with the stability axis yaw rate to form the rudder command. The commanded rudder signal is fed to the yaw jets through an on - off switching logic. The logic turns two aft mounted jets on when the signal equivalent to 4° of rudder is commanded. The commanded rudder signal is also combined with the filtered aileron - rudder interconnect, limited to $\pm 22.8^{\circ}$, and fed to the rudder. The lateral control system gains are presented in table 4.

TEST PROGRAM

The orbiter aerodynamics data of December 1975 were used in this investigation. These data are based on wind tunnel tests using models by Rockwell International Space Division with corrections for configuration changes and operational flight conditions. The force and moment coefficients, as assembled by the orbiter program office (Ref. 1), are based on the wing reference length and area.

Flying Quality Criteria

The flying quality criteria used in this investigation are that a recommended by Donald C. Cheatham, NASA Manned Spacecraft Center, Houston, TX. The vehicle roll accelerations and roll rate requirements were a result of closed loop entry guidance and control studies defining these requirements in order to maintain the vehicle trajectory within acceptable dynamic pressure limits. The roll rate response criterion used has been defined in terms of a roll rate response envelope and is presented in figure 5 for the region of interest for this investigation. The roll rate response due to a step roll rate command of 5 deg/sec shall fall within the response envelope presented. In addition, the criterion of limiting the sideslip to less than 2° during a change in roll attitudes of up to $\pm 45^{\circ}$ was also used. Responses were judged unsatisfactory if roll rate was outside the envelope of figure 5 and/or the sideslip was greater than 2°.

Flight Conditions

Flight condition characteristics for Mach numbers of 1.5 and .6 were obtained for the proposed nominal trajectory, figure 3. Off nominal conditions were computed for the proposed maximum trim α_t uncertainties of $\pm 4^{\circ}$. The condition $\alpha_t = -4^{\circ}$ could not be obtained because of the limits on the maximum dynamic pressure (q_m = 400 lb/ft^2) in the hybrid computer program. To provide as large a variation of angle of attack as possible without exceeding the dynamic pressure limit of the program, angles of attack of 3.5 and 3^o were chosen for the lower boundary off nominal flight condition for Mach numbers of 1.5 and .6, respectively. The flight condition characteristics for the nominal and off nominal trim angles of attack are presented in tables 2 and 3.

Aerodynamic Uncertainties

Variation between wind tunnel and flight aerodynamic derivatives has been noted in existing aircraft; and, in many instances the differences are quite substantial as indicated by Major General Thomas Stafford (AFFTC/Doy) and J. Wiel (DFRC). These differences could cause stability and control problems and are, therefore, a concern in evaluating the handling qualities of the space shuttle orbiter.

Wind tunnel and flight derivatives were correlated for a large number of vehicles; and, a comparison of maximum variations in the derivatives for conventional aircraft and lifting bodies was obtained. Based on statistical consideration, the range of uncertainties in aerodynamic derivatives was established. The recommended increments of the lateral derivative are presented in table 4.

A large number of variations, in single and multiple combinations, were made in the aerodynamic derivative for the augmented configuration. The responses were viewed on a CRT screen and the ones of interest were recorded on a strip chart recorder. The variations included within these recorded cases are of the same magnitude as the predicted uncertainties of table 5 in many cases; in some cases (i.e., β derivatives), the variations are as large as 200 percent of the predicted uncertainties. It was discovered that large variations in the rotary and sideslip derivatives alone have very little effect on the responses. The sideslip derivatives showed some significance in combinations with the control derivatives and are, therefore, included in the cases of interest. A compilation of the selected cases of aerodynamic derivative incremental changes is presented in table 6. The basic and resultant (adding the variation in table 6) values of the aerodynamic characteristics for the configurations investigated are presented in table 7. Table 7 also summarizes the results of each configuration tested.

RESULTS AND DISCUSSION

Unaugmented Configuration

A digital computer program was used to compute the lateral response for a negative 2^o aileron input for the unagumented orbiter at Mach numbers 1.5 and .6 for the nominal angles of attack (α = 6.7^o and α = 4.4^o) and the off nominal angles of attack (α = 3.5^o and α = 3.0^o for the lower boundary; α = 10.8^o and α = 8.5^o for the upper boundary), respectively, to illustrate the need for stability augmentation. The unagumented orbiter responses at Mach 1.5 show a tendency for a roll reversal condition at the higher angle of attack ($\alpha = 10.8^o$) with a large adverse sideslip ($\beta > 2^o$), figure 6. There is an appreciable amount of interaction between the Dutch roll and spiral modes. The roll rate and the sideslip suggest difficulty in controlling the bank angle at the three angles of attack.

At Mach number .6, the response shows that for the lower angles of attack ($\alpha = 3.0^o$ and $\alpha = 4.4^o$) the roll rate reaches 35 deg/sec in less than five seconds with proverse sideslip of about 2^o, figure 7.

Augmented Configuration

A hybrid computer system was programed with six-degree-of-freedom, nonlinear equations of motion to investigate the effects of the aerodynamic uncertainties on the flying qualities of the augmented orbiter. The configuration was augmented with the lateral control system of 1975, figure 5. Time history responses are obtained for a roll rate command of 5 deg/sec for the nominal and off nominal angle of attack conditions. For the Mach number and angle of attack conditions considered, the responses show the roll rate is typical of a first order system, figure 8. Sideslip angles are small ($\beta < .5^o$). At the higher angle of attack conditions ($\alpha = 10.8^o$ and $\alpha = 8.5^o$ for $M = 1.5$ and $M = .6$, respectively) there is an increase in the aileron and rudder deflections. At Mach 1.5, the roll rate response suggests sluggishness for the higher angle of attack condition.

Variations in Aileron and Rudder Derivatives

The responses for the configurations investigated in the study (Table 7) were compared to the responses of the augmented vehicle, figure 8.

The effects of the aileron and rudder control derivative uncertainties are presented in figure 9. Configuration 1, figure 9a, shows a reduced roll rate with some acceleration. Further reduction is seen in the roll rate with an increase in proverse sideslip, aileron, and rudder deflection with an increase in angle of attack (compare Fig. 9a, $\alpha = 6.7^o$, $\alpha = 10.8^o$). Reversal of the roll rate command increases the demand for rudder deflection which requires activation of the yaw jets, as indicated by the data in the rudder channel at the higher angles of attack.

Configuration 2, figure 9b, shows only small or no effects on the response due to aerodynamic uncertainties at the low angle of attack. For configuration 2c (compare Fig. 9b, $\alpha = 8.5^o$), sideslip becomes proverse and the demand on the rudder deflection requires yaw jet activitation with roll rate command input. There is also an increase in yaw jet activitation with reversal of the command. For configuration 3, figure 9c, an unsatisfactory condition exists at the lower angle of attack (3a, $\alpha = 3.5^o$). Even before the roll rate command input was applied, a roll rate developed, i.e., the vehicle began to roll voluntarily. This is why there is an initial roll rate when the control input was applied. Upon application of the control input, the roll rate starts in the right direction but immediately turns around indicating a roll reversal condition.

Configuration 3b ($\alpha = 6.7^{\circ}$) shows a reduction in the roll rate, compared with figure 8, with some oscillation and proverse sideslip. With reversal of the roll rate command, rudder deflections increase and the yaw jet activation is required. For configuration 3c, ($\alpha = 10.8^{\circ}$), rudder demand is high requiring yaw jets with initial roll rate command input. With the reversal of the command, sideslip is large ($\beta \approx 2^{\circ}$) and the rudder deflections become excessive ($\delta r > 10^{\circ}$) with increased yaw jet activation required.

For configuration 4, figure 9d, only a little change from figure 9b is noted at the high angle of attack ($\alpha = 8.5^{\circ}$) where the rudder deflection increases requiring the yaw jets.

Aileron and rudder sideforce uncertainties were considered along with the rolling and yawing moments for the high Mach number and are presented in figure 10. Configuration 5a, ($\alpha = 3.5^{\circ}$) figure 10a, shows a slight increase in the roll rate, compared to figure 8, with some oscillation and a small proverse sideslip. For configuration 5b ($\alpha = 6.7^{\circ}$) the yaw jets were not allowed to fire. For this configuration there is an increase in roll rate oscillations, proverse sideslip and rudder deflections. Upon reversal of the command, there is an increase in sideslip ($\beta \approx 1^{\circ}$) and rudder deflections ($\delta r \approx 6^{\circ}$). For configuration 5c ($\alpha = 10.8^{\circ}$) with roll rate command input, sideslip increases and the demand for rudder deflections greater than 4° requires yaw jets. Upon reversal of the command, large rudder deflections are required ($\delta r > 8^{\circ}$) along with the yaw jet activation and sideslip is large ($\beta \approx 1.8^{\circ}$).

For configuration 6, figure 10b, compare with figure 8a, there is a reduction in the roll rate with some oscillation at the lower angle of attack ($\alpha = 3.5^{\circ}$). Configuration 6b shows an unsatisfactory condition in which roll rate has been reduced to zero. The vehicle would not roll with almost constant aileron and rudder deflection for this roll rate command input. Configuration 6c ($\alpha = 10.8^{\circ}$) would be unsatisfactory in roll because of the reduced roll rate. There is an increase in aileron and rudder deflection with reversal of the roll rate command.

Variation in Aileron, Rudder, and Sideslip Derivatives

The sideslip derivative uncertainties had little or no effect on the lateral responses alone; therefore, they were included with the aileron and rudder derivative uncertainties and are presented in figures 11 and 12. Configuration 7, figure 11a, shows an increase in sideslip oscillations and rudder deflections with yaw jets required as angle of attack increases. For configuration 7c ($\alpha = 10.8^{\circ}$), the demand on the rudder deflection is excessive ($\delta r > 11^{\circ}$) with added requirement on the yaw jets and an increase in sideslip with oscillations. The roll rate shows only a small change from the augmented conditions (Fig. 8a).

Configuration 8, figure 11h, shows only a slight increase in the roll rate, sideslip, and rudder deflections, compared to figure 8b. The aerodynamic uncertainties have very little effect on the response for this condition.

The sideforce derivatives were considered along with the rolling and yawing moment derivatives and the results are shown in figure 12. For configuration 9a, ($\alpha = 3.5^0$) figure 12a, the roll rate is reduced with roll reversal tendencies and proverse sideslip for an unsatisfactory condition. The aileron and rudder deflections are almost constant. Configuration 9b ($\alpha = 6.7^0$) shows sideslip and rudder deflection increases requiring yaw jets with roll rate command inputs. Upon reversal of the command, sideslip and rudder deflection became large ($\beta \approx 2^0$, $\delta r > 8^0$) increasing the requirements for yaw jets. Configuration 9c ($\alpha = 10.8^0$) shows an unsatisfactory condition where the sideslip indicates an aperiodic mode. Roll rate is reduced with roll reversal tendencies and rudder deflection increases. Upon reversal of the command, roll rate is nulled, the rudder deflection is divergent, and the sideslip is limited.

Configuration 10, figure 12b, shows little or no effect due to aerodynamic uncertainties. Configuration 11, figure 12c, shows unsatisfactory responses for all three angles of attack. The roll rate is restrained with constant aileron and rudder deflections at the lower angle of attack ($\alpha = 3.5^0$). The sideslip, the reduced roll rate with roll reversal tendencies, and the divergent rudder deflections indicate an aperiodic mode for the higher angles of attack ($\alpha = 6.7^0$ and $\alpha = 10.8^0$).

CONCLUDING REMARKS

The effects of aerodynamic uncertainties on the handling qualities of the space shuttle orbiter were investigated with the use of six-degree-of-freedom, nonlinear equations of motion on a hybrid computer system. Flight conditions characteristic of Mach numbers of 1.5 and .6 for the nominal and off nominal angle of attack conditions (α's = 3.5^0, 6.7^0, 10.8^0 and α's = 3.0^0, 4.4^0, 8.5^0, respectively), were selected for this investigation. Results revealed that at the low Mach number condition (M = .6) only a few problems exist (i.e., existence of proverse sideslip and an increase in rudder deflection which required the yaw jets) for the angles of attack and the combinations of large aerodynamic variations considered, but not any that would be considered unsatisfactory. At the higher Mach number (M = 1.5) and angle of attack conditions considered, problems resulted from various cases of reduced roll rate, large value of proverse sideslip, and increased rudder deflections and yaw jet activitation with initial roll rate command inputs. Unsatisfactory conditions exist consisting of roll reversal problems and increased proverse sideslip in addition to long periods of large rudder deflections requiring extended use of the yaw jets. There seemed to be an aperiodic mode developing in some instances.

REFERENCES

1. Rockwell International Space Division: Space Shuttle Program, Aerodynamic Design Data Book, Vol. 1, Orbiter Vehicle, December 1975.

Table 1. Space Shuttle Orbiter Mass and Physical Characteristics

Weight, N (lb)	807123.5 (181449)
c.g., percent body length	66.25
Moments of inertia	
I_x, Kg - m^2 (slug-ft^2)	1169242.6 (863384.6)
I_y	8729442.66 (6438473
I_z	8991817.8 (6631990)
I_{xz}	-218616.2 (-161242.2)
Wing Dimensions	
Span, m (ft)	23.793 (78.06)
Area, m^2 (ft^2)	249.63 (2690)
Cord, m (ft)	12.06 (39.57)
Surface Deflection Limits	
Elevons, deg	-35, +20
Rudder, deg	-228, +22.8
Speed Brakes, deg	-87.2, 0
Body Flaps, deg	-11.7, +16.3

Table 2. Flight Conditions Characteristic for Mach Number 1.5

h, ft	50,000	62,000	70,000
V, ft/sec	1,452.1	1,529.56	1,456.35
$\bar{q}$, #/ft^2	383.68	239.86	147.62
α, deg	3.5	6.7	10.8
θ, deg	-19.5	-6.68	-8.24
C_{l_β}, per rad	-.0875	-.087	-.0883
C_{l_p}, per rad	-.293	-.284	-.307
C_{l_r}, per rad	.103	.115	.138
C_{n_β}, per rad	.0375	.019	.00619
C_{n_p}, per rad	.158	.133	.113
C_{n_r}, per rad	-.453	-.433	-.384
C_{y_β}, per rad	-.955	-.946	-.968
$C_{l_{\delta a}}$, per rad	.0897	.081	.0841
$C_{l_{\delta r}}$, per rad	.034	.031	.0307
$C_{n_{\delta a}}$, per rad	-.0036	.008	.008
$C_{n_{\delta r}}$, per rad	-.059	-.056	-.055
$C_{y_{\delta a}}$, per rad	-.0183	-.018	-.01445
$C_{y_{\delta r}}$, per rad	.112	.103	.1014

Table 3. Flight Conditions Characteristic for Mach Number .6

h, ft	9,000	18,000	33,000
V, ft/sec	648.82	627.08	589.13
$\bar{q}$, #/ft^2	381.257	266.484	138.234
α, deg	3.0	4.4	8.5
θ, deg	-19.3	-18.7	-13.8
C_{l_β}, per rad	-.077	-.093	-.123
C_{l_p}, per rad	-.277	-.282	-.309
C_{l_r}, per rad	.144	.153	.179
C_{n_β}, per rad	.109	.095	.09
C_{n_p}, per rad	.198	.188	.159
C_{n_r}, per rad	-.263	-.262	-.305
C_{y_β}, per rad	-1.135	-1.125	-1.081
$C_{l_{\delta a}}$, per rad	.210	.215	.225
$C_{l_{\delta r}}$, per rad	.047	.046	.044
$C_{n_{\delta a}}$, per rad	.033	.031	.034
$C_{n_{\delta r}}$, per rad	-.082	-.078	-.073
$C_{y_{\delta a}}$, per rad	-.180	-.187	202
$C_{y_{\delta r}}$, per rad	.162	.157	.144

Table 4. Space Shuttle Orbiter Lateral Control System Gains

Mach No.	.6		.6	1.5		1.5
h, ft.	9,000	18,000	33,000	50,000	62,000	70,000
, deg.	3.0	4.4	8.5	3.5	6.7	10.8
KP1	1	1	1	1	1	1
KP2	.543	.543	.543	.543	.658	.543
KP3	.393	.563	.970	.391	.625	.970
KR1	5.9	5.9	5.9	5.9	5.9	5.9
KR2	.472	.675	.850	.469	.75	.850
KR3	.0	.0	.0	.1455	.3731	.7223
KNY	.419	.419	.419	1.11	1.233	1.11
KJI	.25	.25	.25	.25	.25	.25

Table 5. Suggested Space Shuttle Orbiter Lateral Aerodynamic Uncertainties Incremental Range

Mach No.	.25	.6	.8	1.05	1.2	1.5	2	3	4	5	8	10
C_{n_β}, 1/deg	.0005	.00053	.0008	.00085	.00081	.00058	.00043	.00039	.00043	.00049	.0006	.0006
C_{ℓ_β}, 1/deg	.00084	.00085	.0009	.001	.001	.00095	.0008	.00049	.00038	.00036	.00035	.0006
C_{y_β}, 1/deg	.006	.006	.006	.00598	.00594	.00577	.0053	.00438	.0036	.00303	.0028	.00035
$C_{\ell_{\delta a}}$, 1/deg	.00096	.0009	.00079	.00065	.00056	.00046	.00037	.00031	.00032	.00033	.00035	.0028
$C_{n_{\delta a}}$, 1/deg	.0006	.0006	.0006	.0006	.0006	.0006	.0005	.0005	.00034	.00032	.00032	.00035
$C_{\ell_{\delta r}}$, 1/deg	.000409	.000409	.000409	.000409	.000408	.00035	.000166	.00015	.00015	.00015	.00015	.00032
$C_{n_{\delta r}}$, 1/deg	.00039	.0004	.00047	.0006	.00059	.0005	.00048	.00038	.00038	.00038	.00038	.00015
$C_{y_{\delta r}}$, 1/deg	.001	.001	.001	.000984	.00095	.0008	.00056	.00039	.00031	.00027	.0002	.00017
C_{ℓ_p}, deg/sec	.1					.1						.1
C_{n_p}, deg/sec	.2					.2	.1					.1
C_{ℓ_r}, deg/sec	.1					.1						.1
C_{n_r}, deg/sec	1.	1.	.2				.2	1.				1.

Table 6. Lateral Derivatives Incremental Changes

Conf.	Mach No	[illegible] deg.	[illegible] 1/deg	$C_{n_{\delta a}}$ 1/deg	[illegible]a 1/deg		[illegible] 1/deg	[illegible] r 1/deg	-y[illegible]r 1/deg		[illegible] 1/deg	C_n[illegible] 1/deg	[illegible] 1/deg
1 a	1.5	3.5	.0003	-.0003			.0006	.0006					
b		6.7	.0003	-.0003			.0007	.0007					
c		10.8	.0003	-.0003			.0007	.0007					
2 a	.6	3.0	.000904	-.000603			.000601	.000601					
b		4.4	.000908	-.000606			.000808	.000808					
c		8.5	.0009	-.0006			.000606	.000606					
3 a	1.5	3.5	.000403	-.000403			.0006	.0006					
b		6.7	.0006	-.0006			.0005	.0005					
c		10.8	.0003	-.0003			.00071	.00071					
4 a	.6	3.0	.000901	-.0006			.000601	.000601					
b		4.4	.0009	-.0006			.0008	.0008					
c		8.5	.000904	-.000602			.000601	.000601					
5 a	1.5	3.5	.000419	-.000502	.00067		.000406	.000507	-.000812				
b		6.7	.00043	-.000516	.000688		.000403	.000504	-.000806				
c		10.8	.000508	-.000609	.000812		.000411	.000513	-.000821				
6 a	1.5	3.5	-.0004	-.0004	.0009		.000406	.000507	-.000912				
b		6.7	-.000406	-.000406	.000731		.000504	.000605	-.000907				
c		10.8	-.000402	-.000402	.000724		.000403	.000403	-.000906				
7 a	1.5	3.5	.000402	-.000403			.000601	.000601			.000603	-.000603	
b		6.7	.0005	-.0005			-.0005	.0005			.0006	-.0006	
c		10.8	.0005	-.0005			.000519	.000519			.0005	-.0005	
8 a	.6	3.0	.000904	-.000605			.000901	.000901			.00091	-.000607	
b		4.4	-.000907	-.000604			.000601	.000601			.000918	-.00051	
c		8.5	-.000904	-.000602			.000606	.000606			.000906	-.000504	
9 a	1.5	3.5	.000417	-.0005	.000668		.000481	.000602	-.000963		.001001	-.000601	.006005
b		6.7	.000419	-.000504	-.00067		.00056	.000707	-.001123		.001	-.0006	.006
c		10.8	-.000401	-.000481	.000641		.000505	.000707	-.001131		-.001015	-.000609	.00609

Table 6. Concluded

Conf.	[illegible]	deg.	[illegible] 1/deg	[illegible] 1/deg	[illegible] 1/deg	[illegible] 1/deg	[illegible] 1/deg	[illegible] 1/deg	[illegible] 1/deg	[illegible] 1/deg	[illegible] 1/deg
10 a	.6	3.0	-.000907	-.000604	.001007	.000607	.000607	-.001012	-.00091	-.000506	.006067
b		4.4	-.000904	-.000603	.001004	-.000601	.000601	-.001002	-.000912	-.000507	.006078
c		8.5	.000905	-.000604	.001006	-.000805	.000804	-.001341	-.0091	.000506	-.006067
11 a	1.5	3.5	-.000404	-.000404	.000908	.0004	.0005	-.000899	.000908	-.000505	.006054
b		6.7	-.0006	-.0006	.0008	-.000565	.000706	-.00113	-.001015	-.000609	.006089
c		10.8	.000585	-.000703	.000937	-.000484	.000605	-.000968	-.001004	-.000603	.00603

ORIGINAL PAGE IS OF POOR QUALITY

Table 7. Basic Aerodynamic Derivatives and the Effective Changes

Config.	Condition	Mach No.	deg.	$C_{l_{\delta a}}$ 1/rad	$C_{n_{\delta a}}$ 1/rad	$C_{y_{\delta a}}$ 1/rad	$C_{l_{\delta r}}$ 1/rad	$C_{n_{\delta r}}$ 1/rad	$C_{y_{\delta r}}$ 1/rad	C_{l_β} 1/rad	C_{n_β} 1/rad	C_{y_β} 1/rad
				Basic Aerodynamic Derivatives								
		1.5	3.5	.0897	-.0036	-.01832	.034	-.059	.112	-.0875	.0375	-.955
			6.7	.081	.008	-.018	.031	-.056	.103	-.087	.019	-.946
			10.8	.0841	.008	-.01445	.0307	-.055	.1014	-.0883	.00619	-.968
		.6	3.0	.210	.033	-.180	.047	-.082	.162	-.077	.109	-1.135
			4.4	.215	.031	-.187	.046	-.078	.157	-.093	.095	-1.125
			8.5	.225	.034	-.202	.044	-.073	.144	-.123	.09	-1.081
				Effective Aerodynamic Derivatives								
1a	RR,SP	1.5	3.5	.10689	-.02079		.06838	-.02462				
b	RR,SP,JWRI		6.7	.09819	-.00919		.07111	-.01589				
c	PHRT,SP,JWRI		10.8	.10129	-.00919		.07081	-.01489				
2a		.6	3.0	.2618	-.00155		.08144	-.04756				
b			4.4	.26703	-.00372		.07872	-.03828				
c	SP,JWI,JWRI		8.5	.27657	-.00038		.07872	-.03828				
3a	UNS,PHR,SP	1.5	3.5	.06661	-.02669		.06838	-.02462				
b	RR,SP,JWRI		6.7	.11538	-.02638		.05965	-.02735				
c	UNS,SL,RDL, JWI,JWRI		10.8	.10129	-.00919		-.00998	-.01432				
4a		.6	3.0	.15837	-.00138		.01256	-.04756				
b			4.4	.26657	-.00338		.00016	-.03216				
c	SP,JWRI		8.5	.1732	-.00049		.07844	-.03856				
5a	SP,JWRI	1.5	3.5	.11371	-.03236	.02007	.01074	-.02995	.06547			
b	SP,RDL		6.7	.10564	-.02157	.02142	.00791	-.02712	.04682			
c	SP,RDL,JWI, JWRI,SL		10.8	.11321	-.0269	.03208	.00715	-.02561	.05436			

Abbreviations

- RR - reduced roll rate
- SP - sideslip proverse
- JWI - yaw jets with initial commanded roll rate
- JWRI - yaw jets with reverse roll rate command
- PHR - roll reversal
- SL - sideslip large
- RDL - large rudder deflection
- PHRT - tendency to roll reversal
- UNS - unsatisfactory

Table 7. Concluded

Config.	Condition	Mach No.	α, deg.	$C_{l_{\delta a}}$ 1/rad	$C_{n_{\delta a}}$ 1/rad	$C_{y_{\delta a}}$ 1/rad	$C_{l_{\delta r}}$ 1/rad	$C_{n_{\delta r}}$ 1/rad	$C_{y_{\delta r}}$ 1/rad	C_{l_β} 1/rad	C_{n_β} 1/rad	C_{y_β} 1/rad
6a	RR	1.5	3.5	.06678	-.02652	.03325	.01074	-.02995	.05974			
b	UNS,P=0		6.7	.05774	-.01526	.02389	.05988	-.02133	.05103			
c	UNS,RR		10.8	.06107	-.01503	.02704	.05379	-.03191	.04949			
7a	SP,JWRI	1.5	3.5	.11273	-.02669		-.00044	-.02456		-.05295	.00295	
b	SP,JWI,JWRI		6.7	.10965	-.02065		.00235	-.02735		-.05262	-.01538	
c	UNS,SP,RDL, JWI,JWRI,SL		10.8	.11275	-.02065		.00096	-.02526		-.05965	-.02246	
8a		.6	3.0	.2681	-.00167		.09863	-.03037		-.02486	.07422	
b			4.4	.16303	-.00361		.08044	-.04356		-.0404	.06578	
c	SP		8.5	.1732	-.00049		.00928	-.03828		-.07108	.06112	
9a	UNS,SP,PHRT, JWRI	1.5	3.5	.11359	-.03225	.01996	.06156	-.02451	.05682	-.03014	.00306	-.61091
b	UNS,SP,JWI, JWRI,SL		6.7	.10501	-.02088	.02039	-.00109	-.01549	.03865	-.0297	-.01538	-.6022
c	UNS,PHRT,SL, JWI,JWRI		10.8	.06112	-.01959	.02228	.00176	-.01449	.03659	-.03014	-.02871	-.6190
10a		.6	3.0	.15803	-.00161	-.1223	.08178	-.04722	.10401	-.12914	.08001	-.78736
b			4.4	.1632	-.00355	-.12947	.01156	-.04356	.00959	-.14526	.06595	-.77673
c			8.5	.27686	-.00061	-.14436	-.00213	-.02693	.06716	-.07514	.06101	-.73336
11a	UNS,P 0	1.5	3.5	.06655	-.02675	.03371	.05692	-.03035	.06049	-.03547	.00856	-.6081
b	UNS,RDL,SL, JWRI,PHRT		6.7	.04662	-.02638	.02784	-.00137	-.01555	.03825	-.14516	-.0159	-.5971
c	UNS,RDL,SL, JWI,JWRI,PHRT		10.8	.11762	-.03228	.03924	.00297	-.02033	.04593	-.14583	-.02836	-.6225

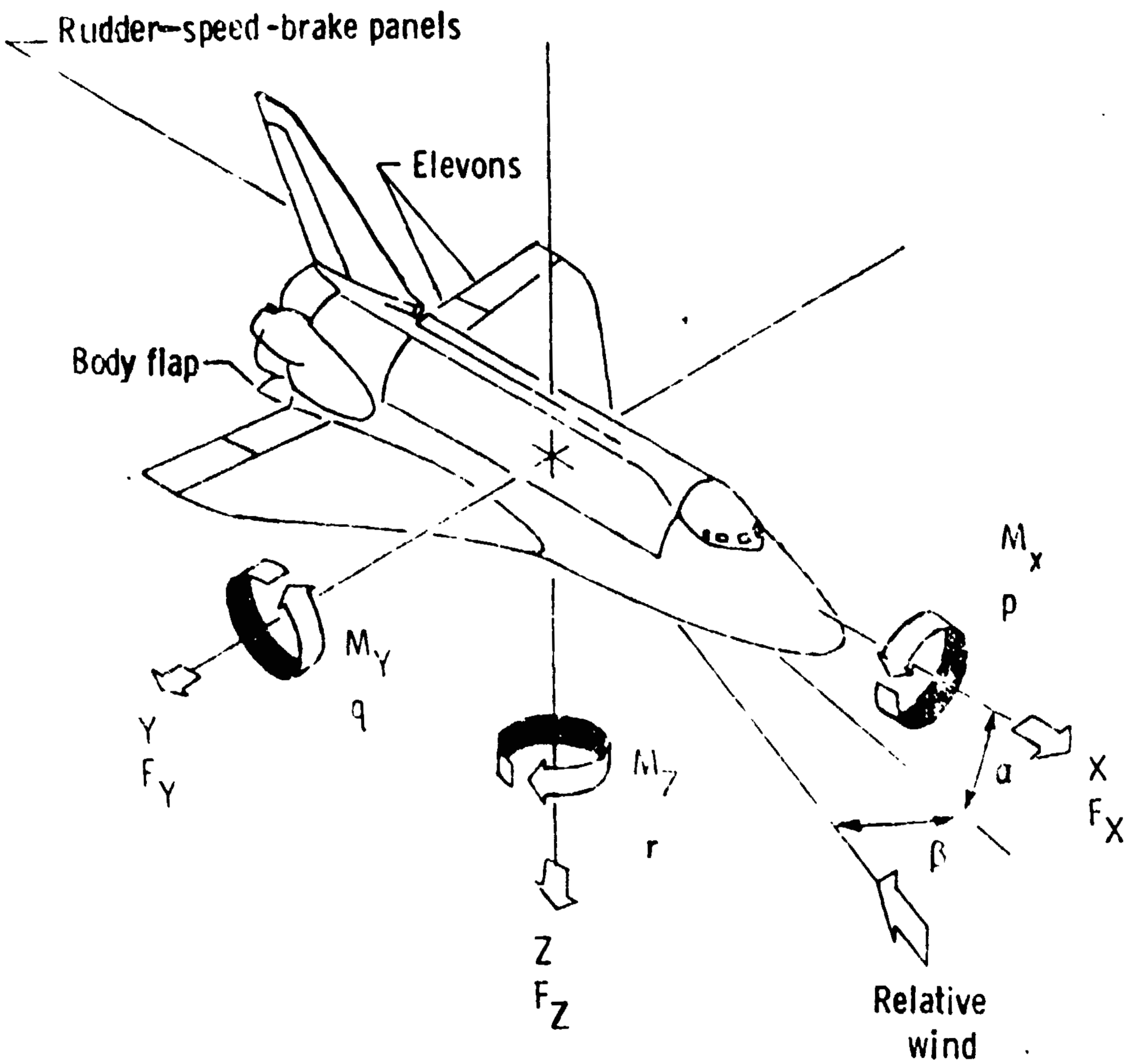

Figure 1.- System of body axes used. Positive directions are indicated.

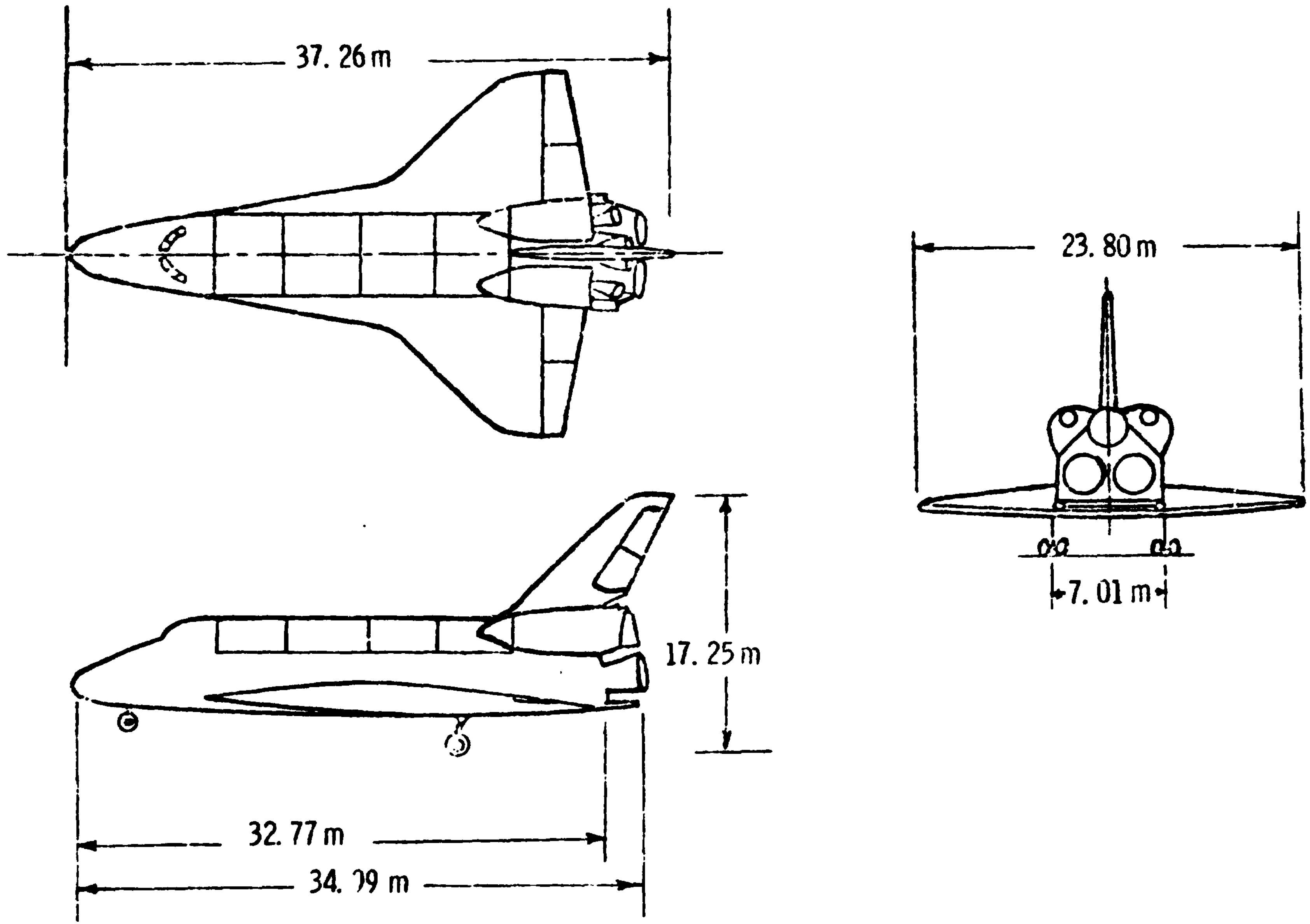

Figure 2.- Three view drawing of the space shuttle orbiter.

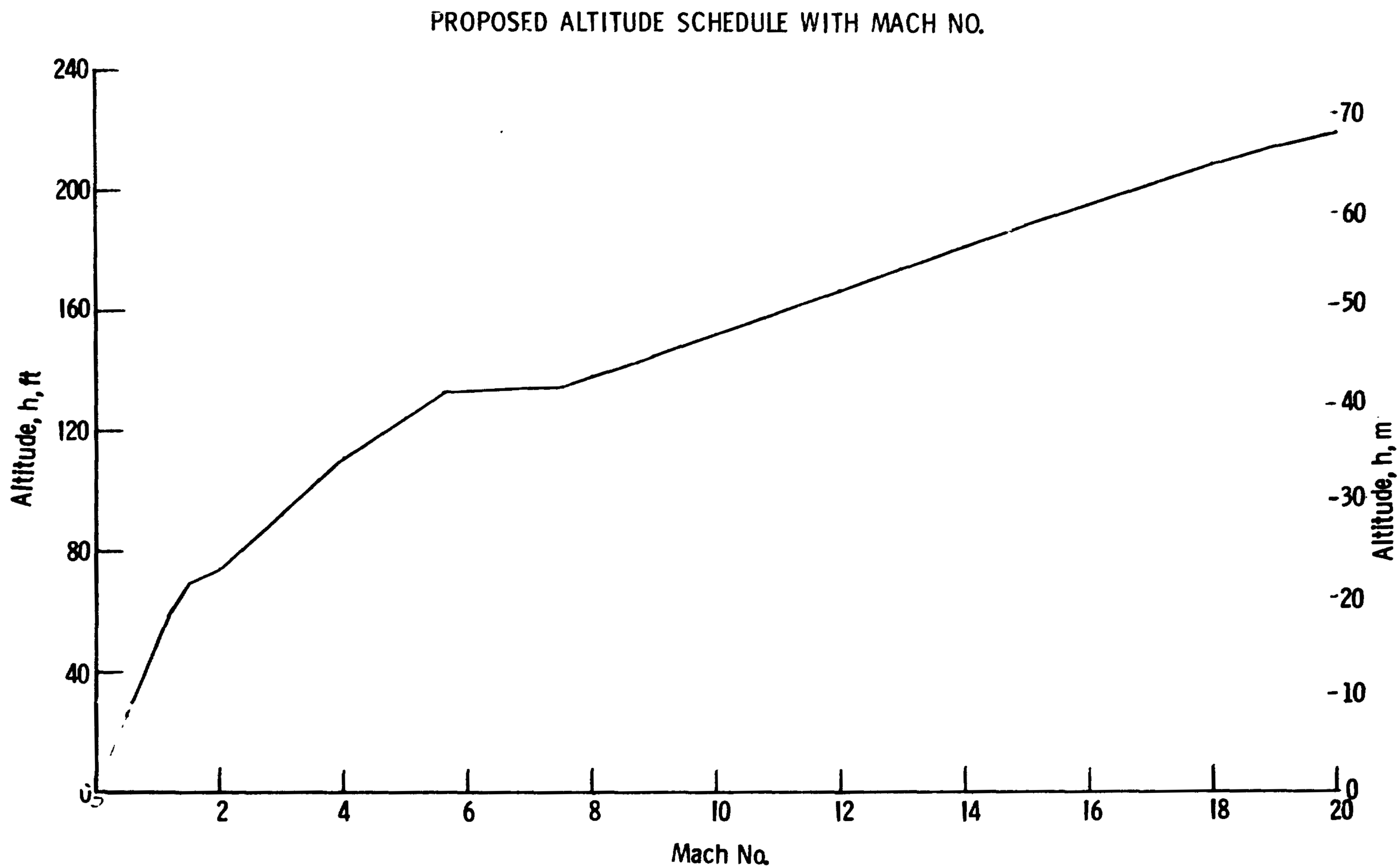

Figure 3.- Proposed altitude schedule with Mach number.

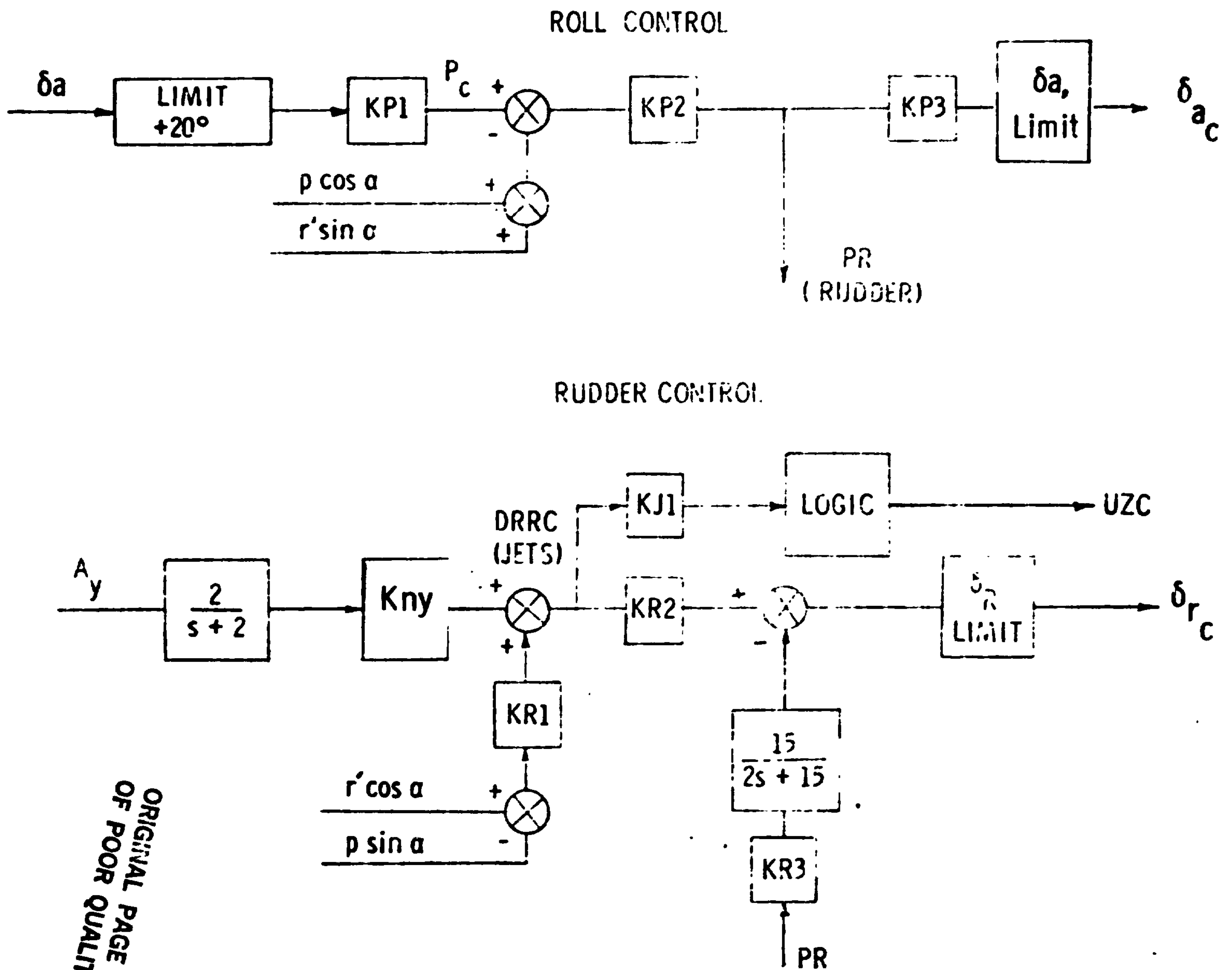

Figure 4.- Space shuttle orbiter lateral control system.
(late system)

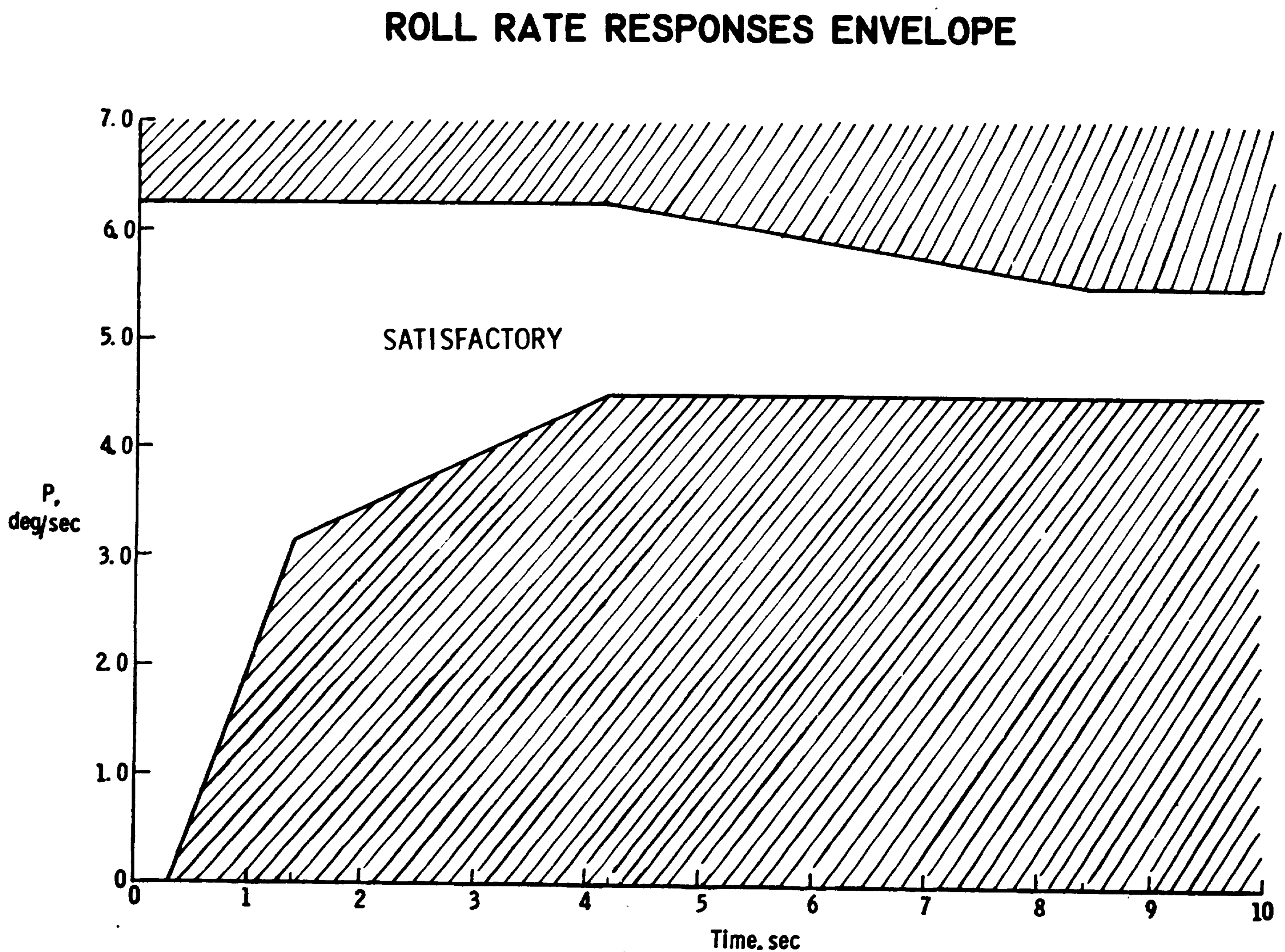

Figure 5.- Space shuttle orbiter satisfactory roll rate

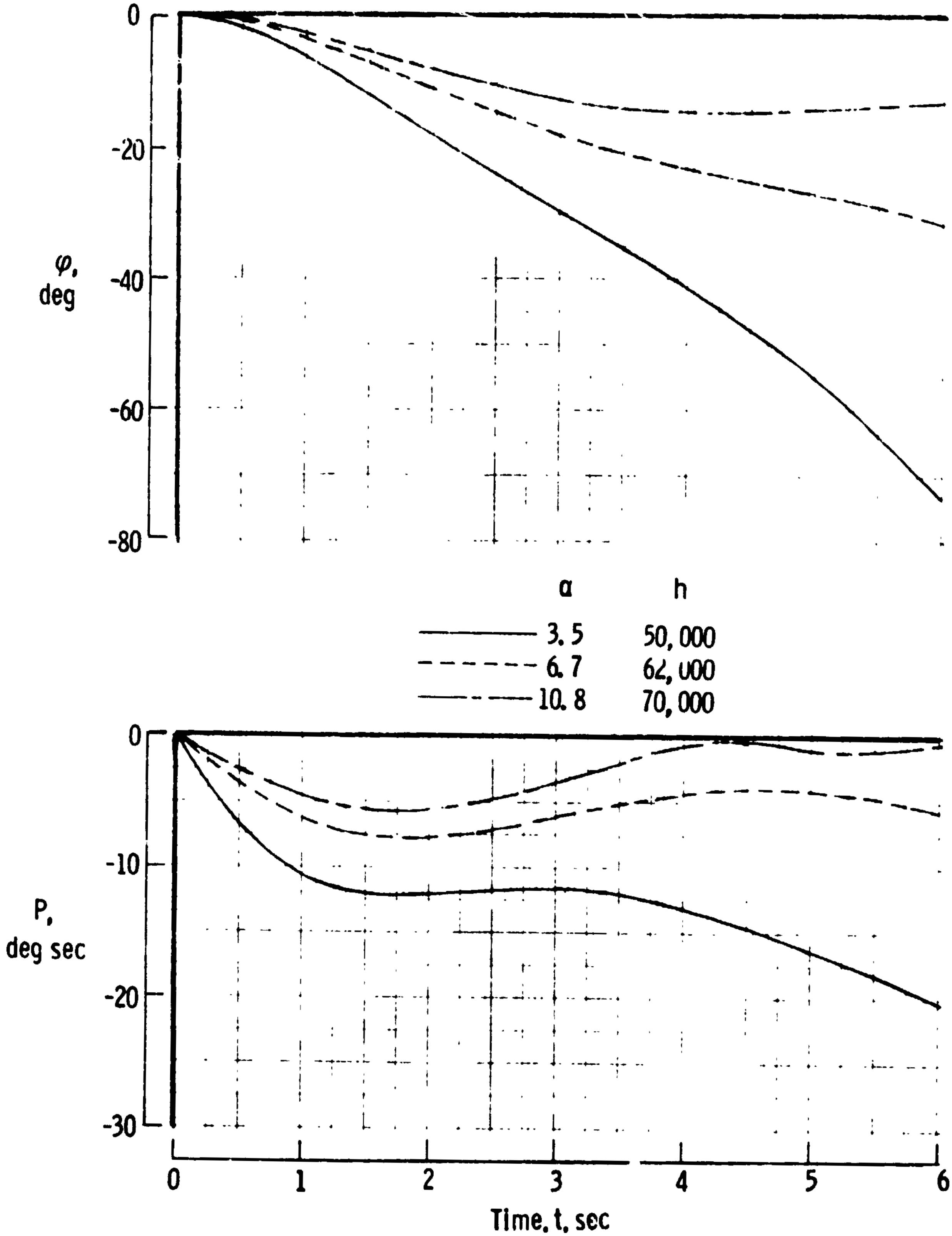

(a) Mach number 1.5

Figure 6.- Response for the unagumented space shuttle orbiter for a two degree aileron input.

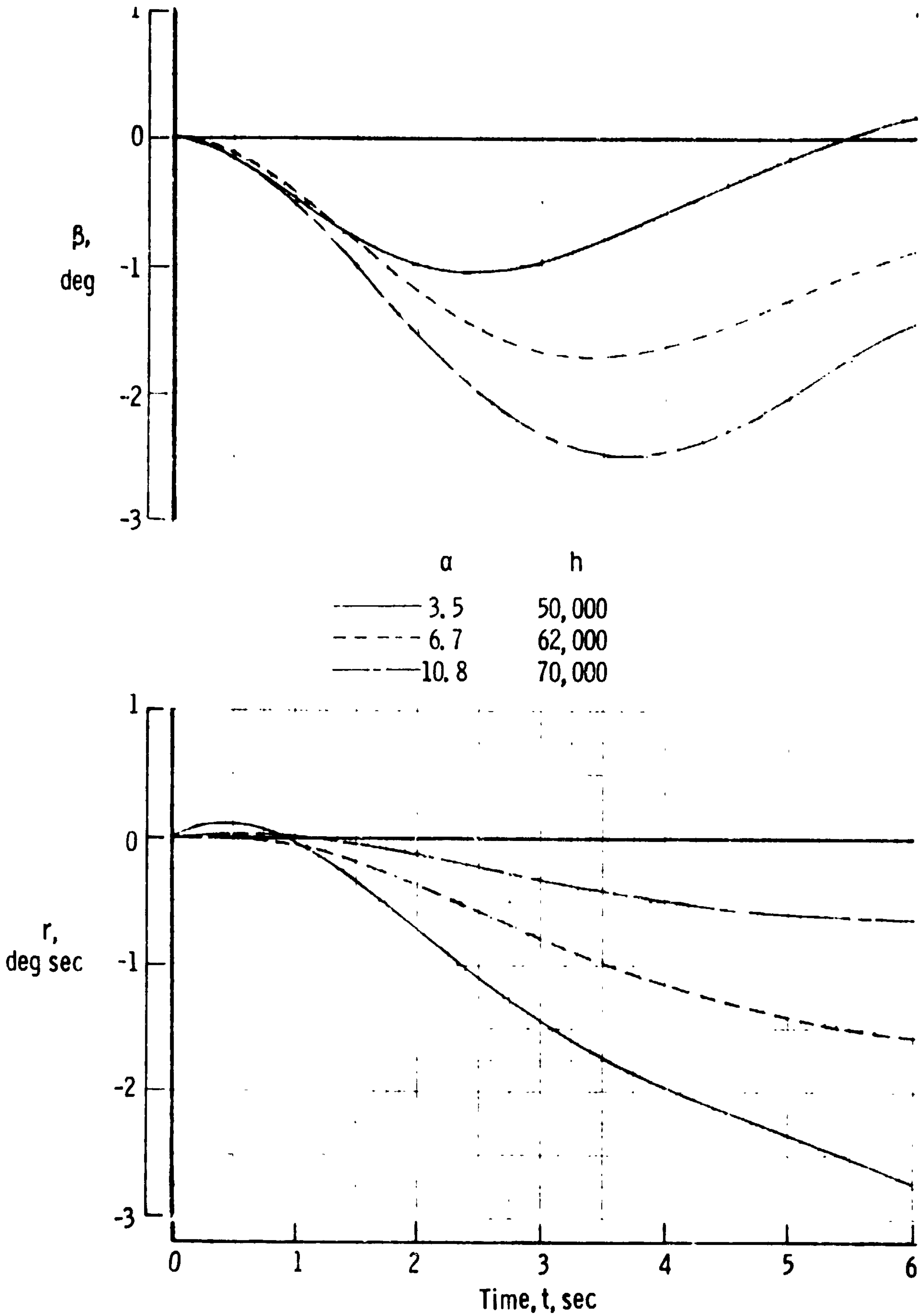

(b) Mach number 1.5

Figure 6. Concluded.

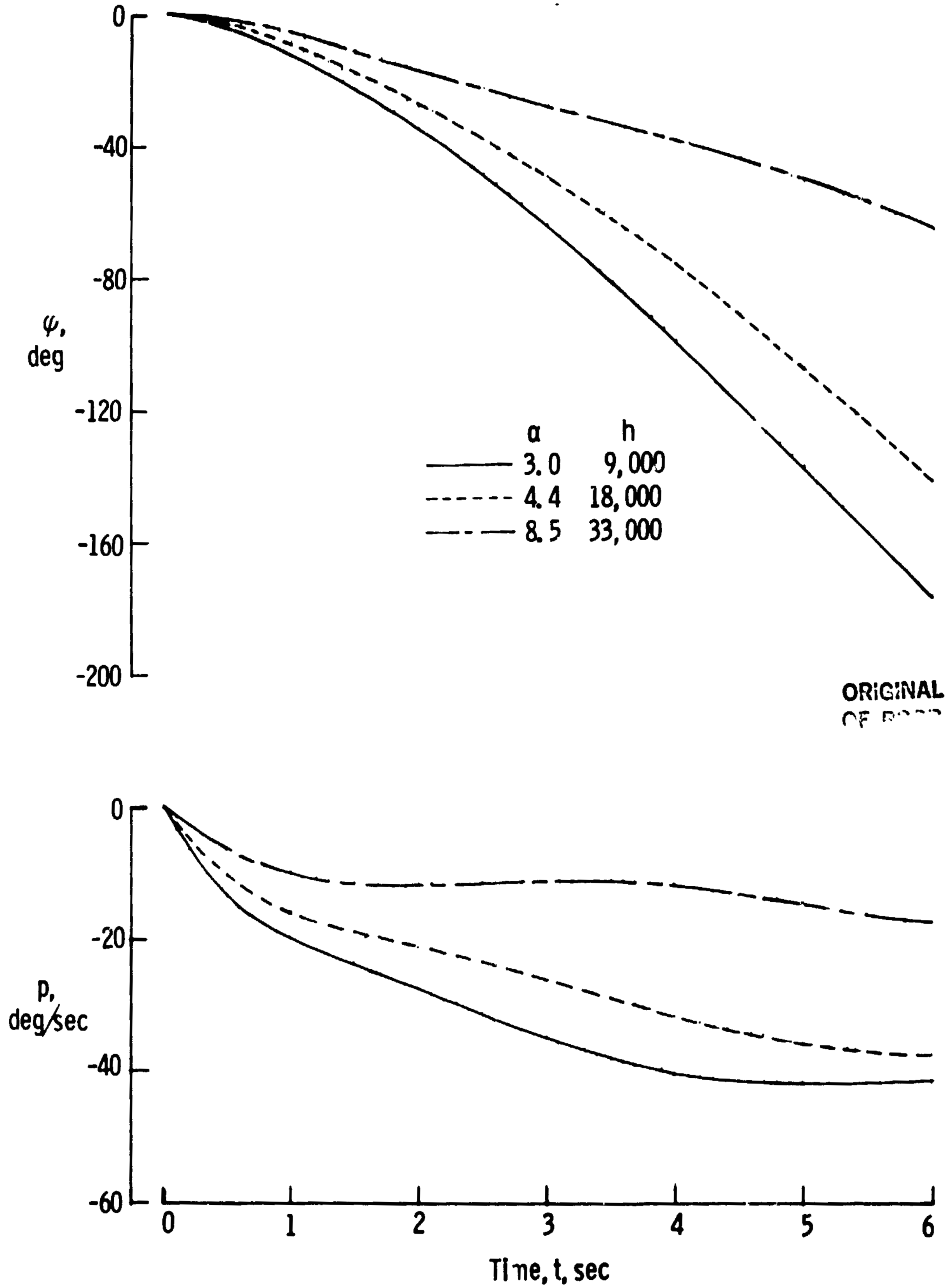

ORIGINAL PAGE IS
OF POOR QUALITY

(a) Mach number .6

Figure 7.- Response for the unaugmented space shuttle orbiter for a two degree aileron input.

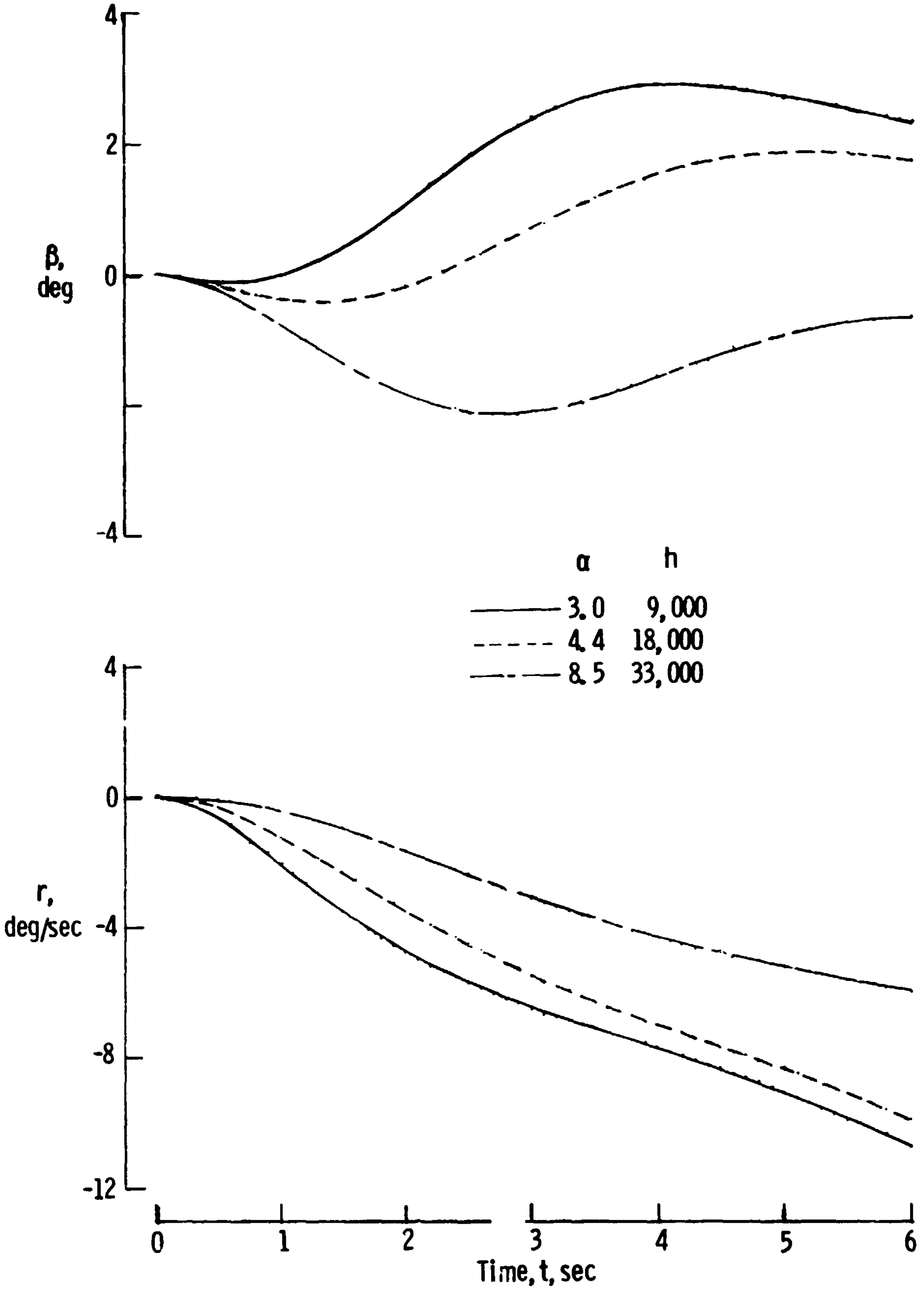

(b) Mach number .6

Figure 7.- Concluded.

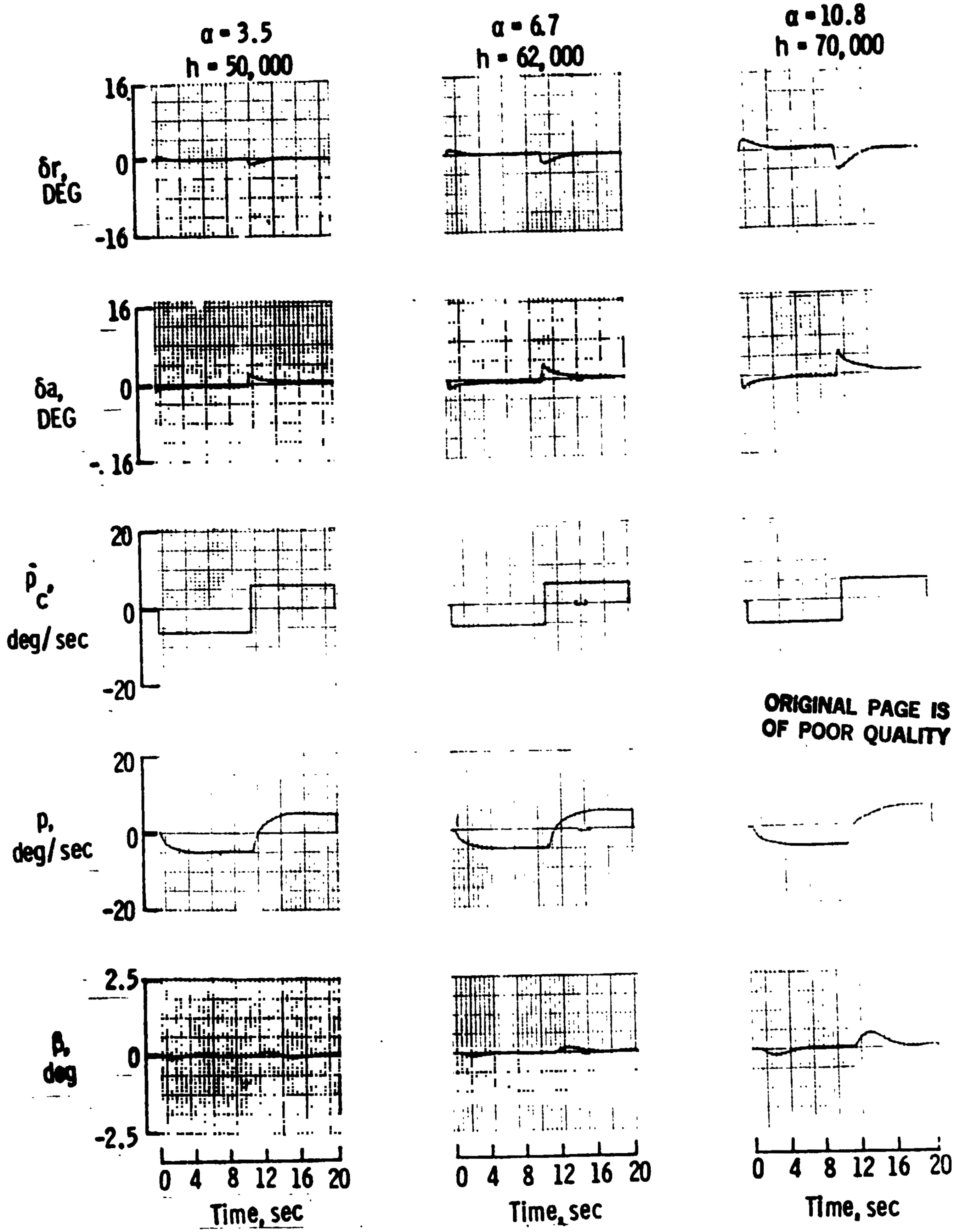

ORIGINAL PAGE IS OF POOR QUALITY

(a) Mach number 1.5

Figure 8.- Response for the augmented space shuttle orbiter for a five deg/sec roll rate command.

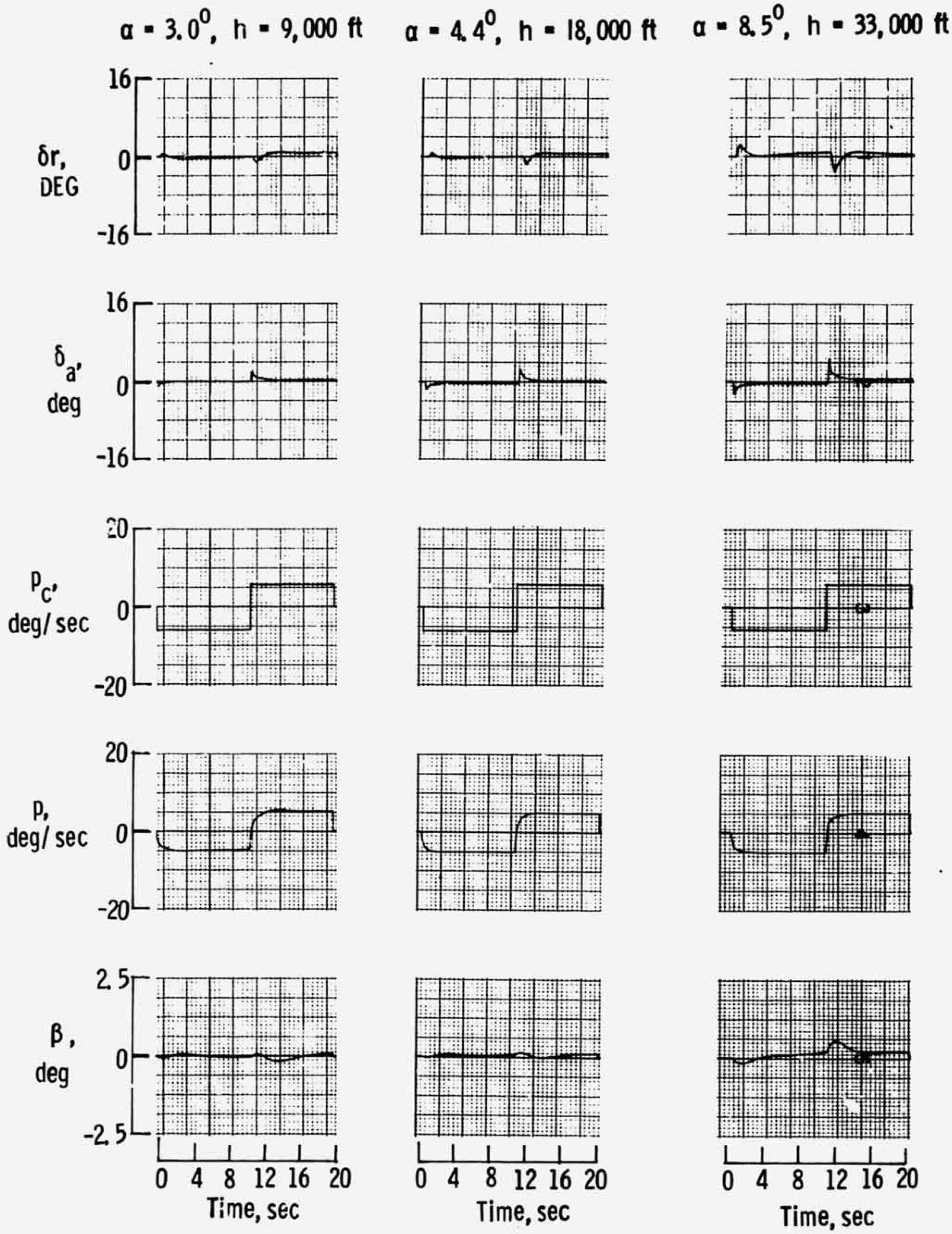

(b) Mach number .6

Figure 8.- Concluded.

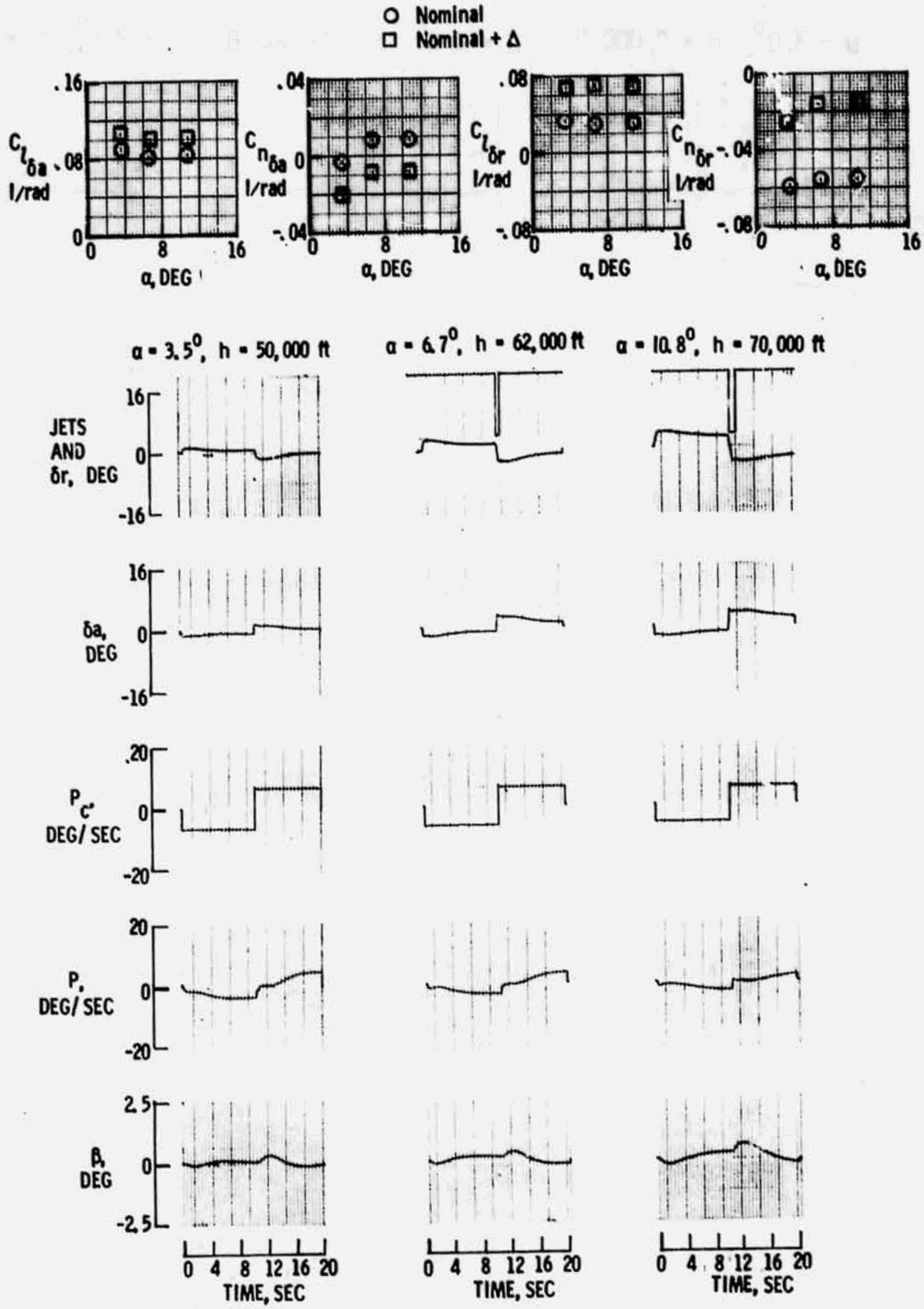

(a) Mach number 1.5

Figure 9.- The effects of variations in the aileron and rudder rolling and yawing moments for a five deg/sec roll rate command.

ORIGINAL PAGE IS
OF POOR QUALITY

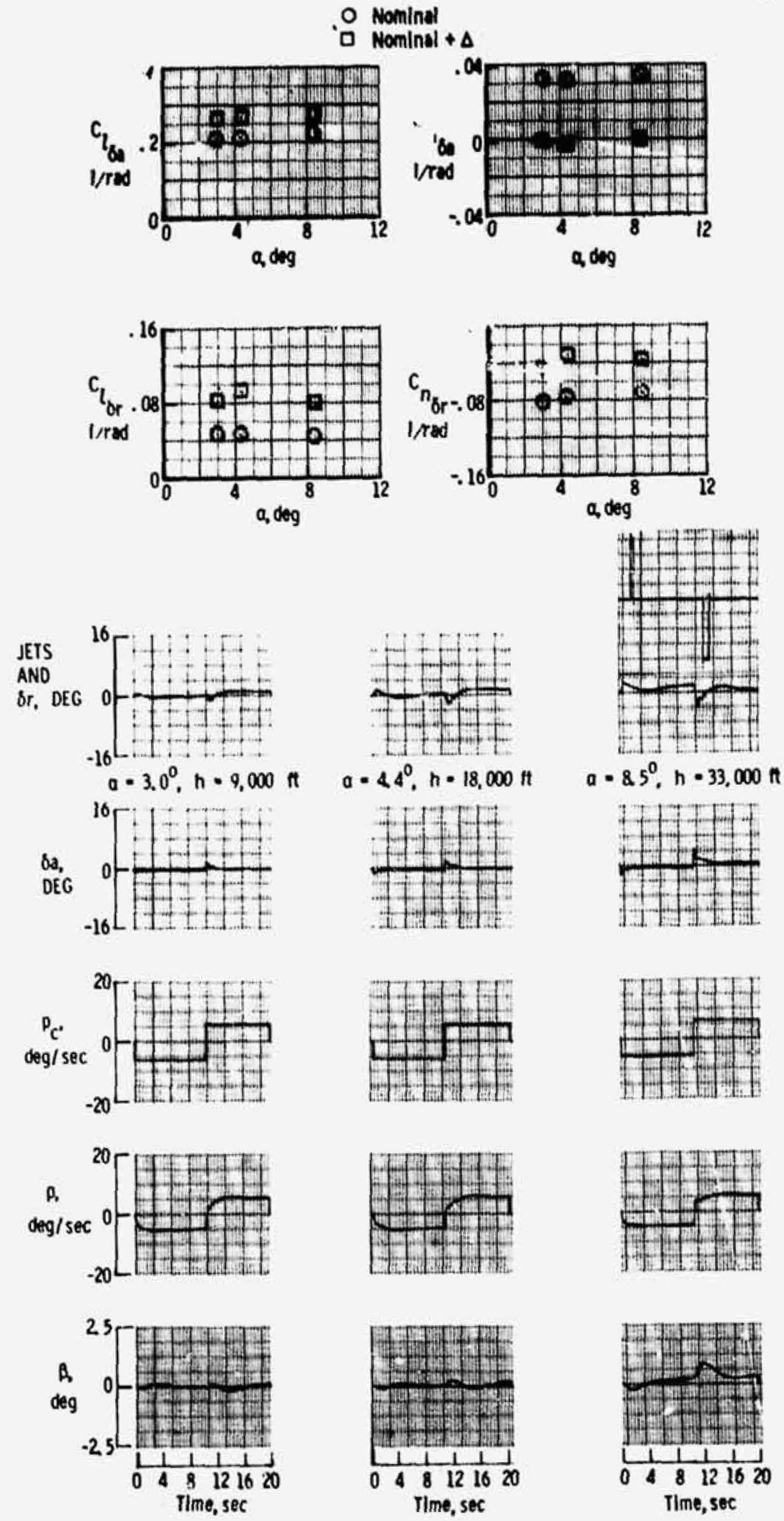

(b) Mach number .5

Figure 9.- Continued.

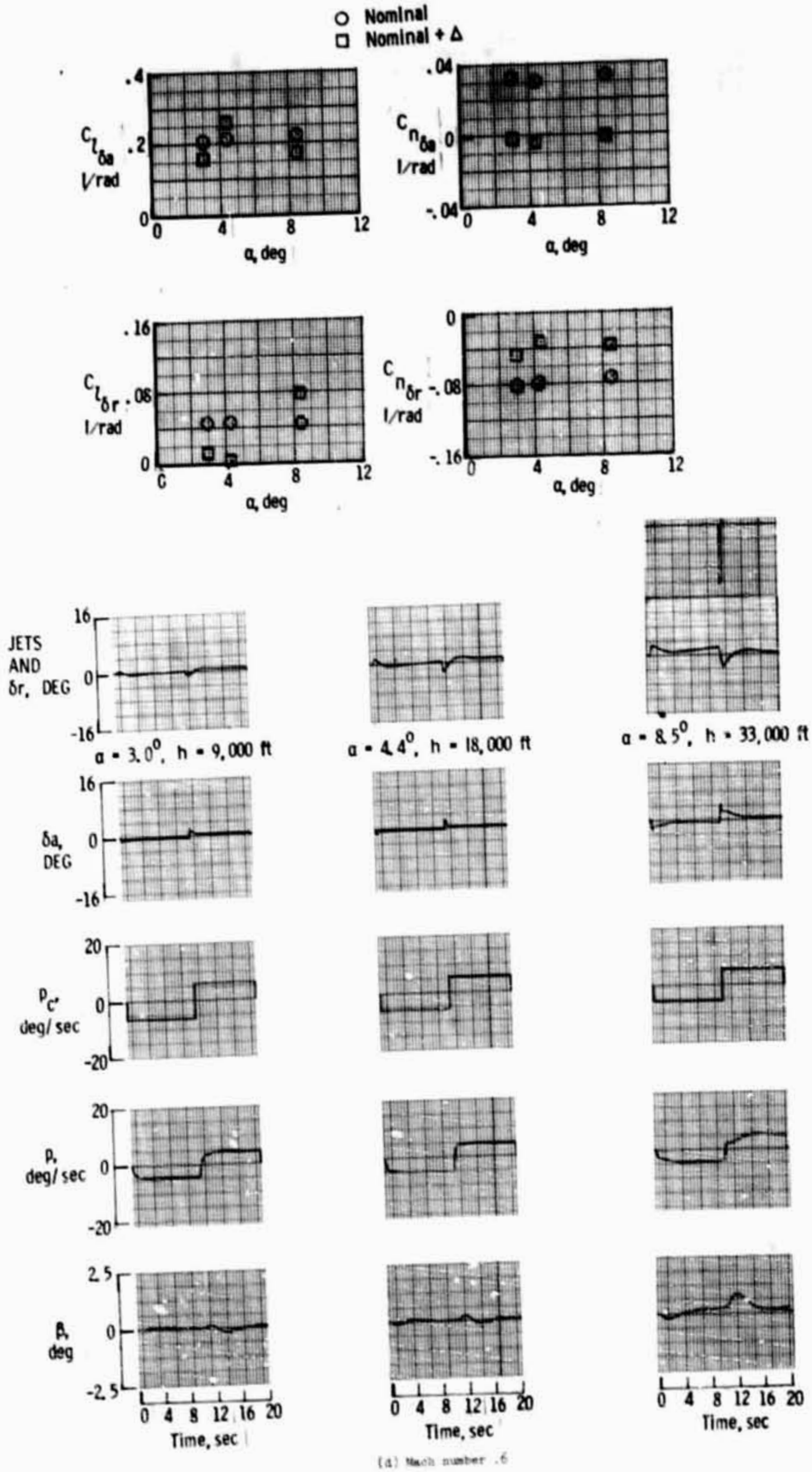

(d) Mach number .6

Figure 9.- Concluded.

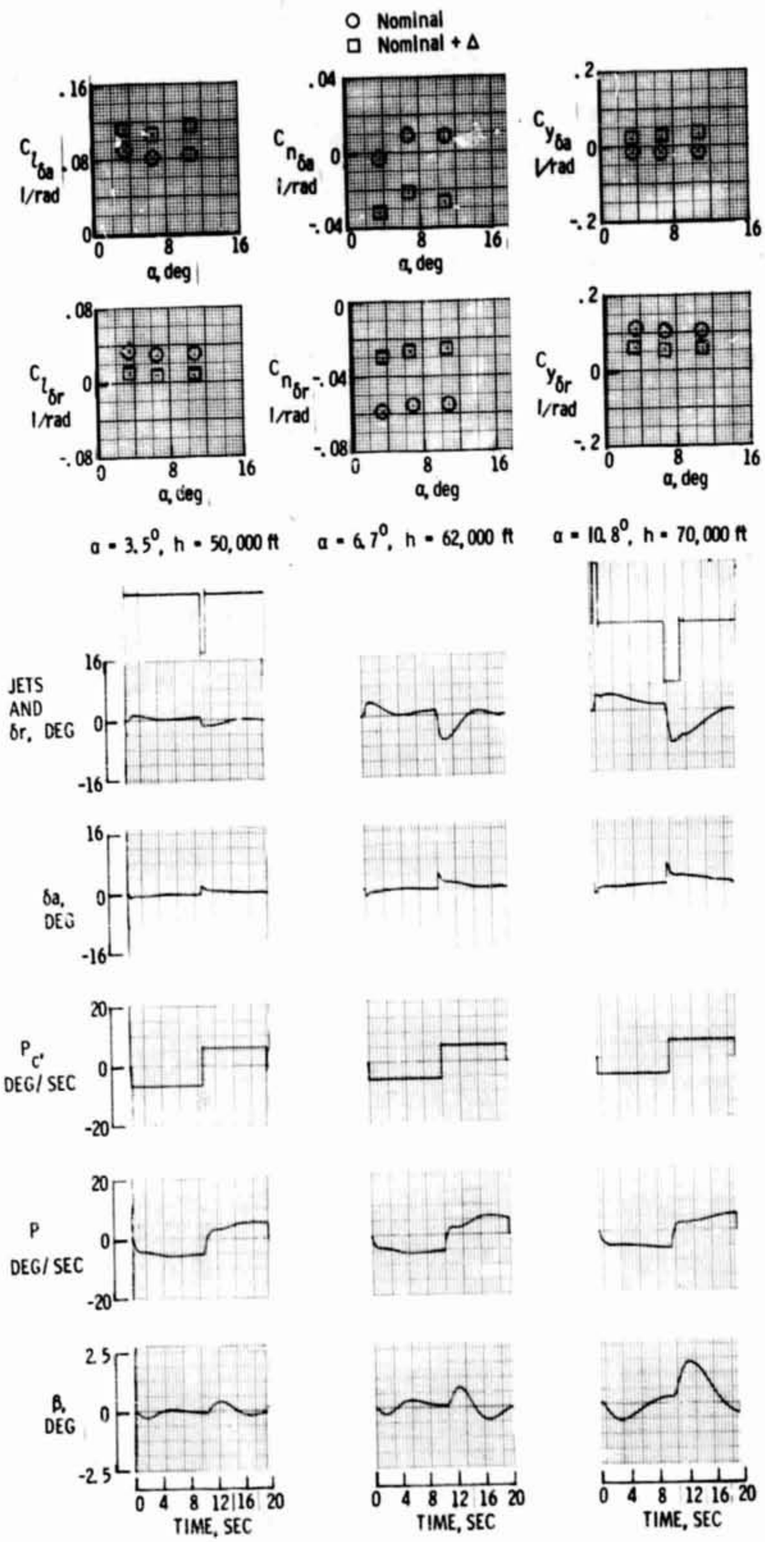

(a) Mach number 1.5

Figure 10.- The effects of variations in the aileron and rudder rolling and yawing moments and side forces.

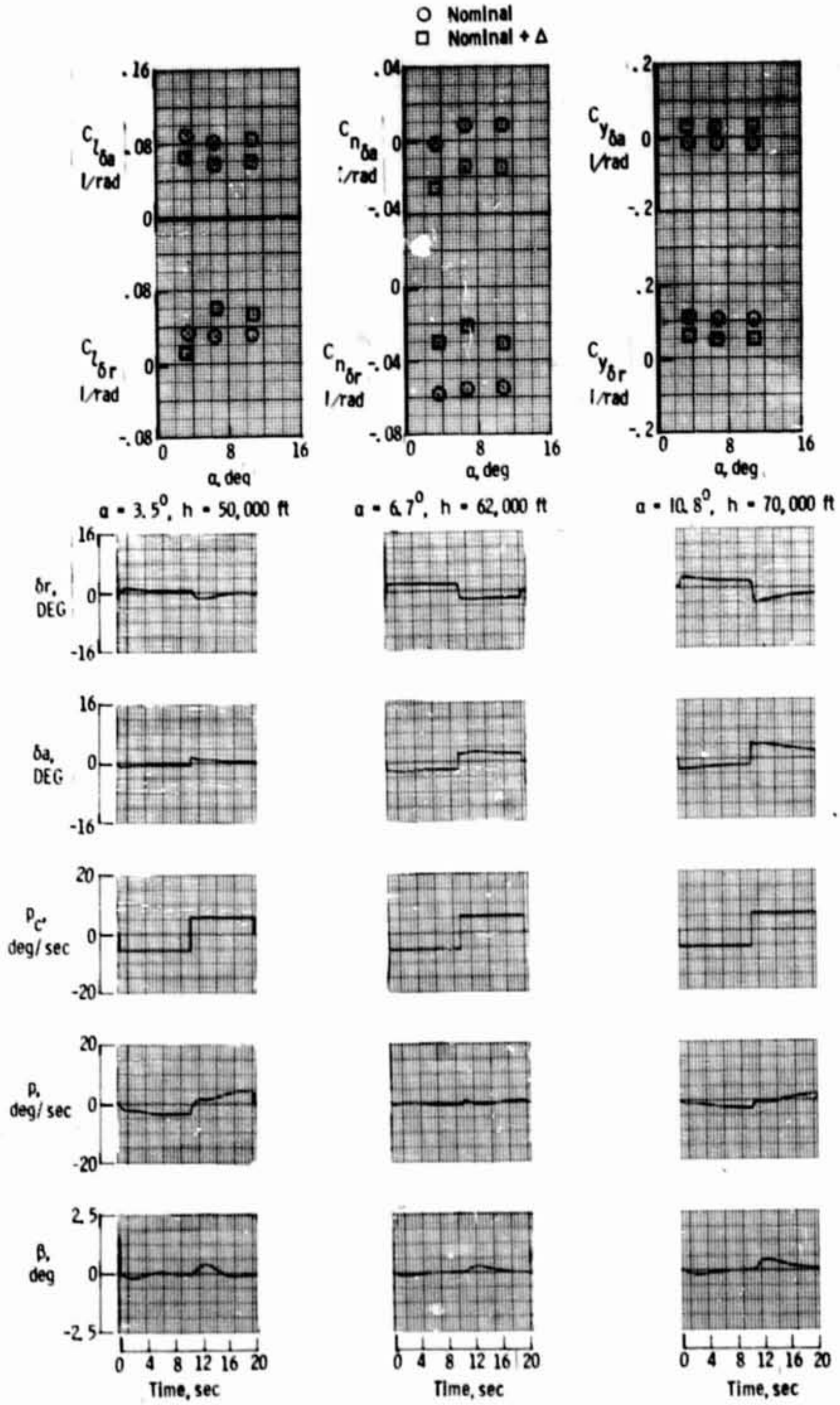

(b) Mach number 1.5

Figure 10.- Concluded.

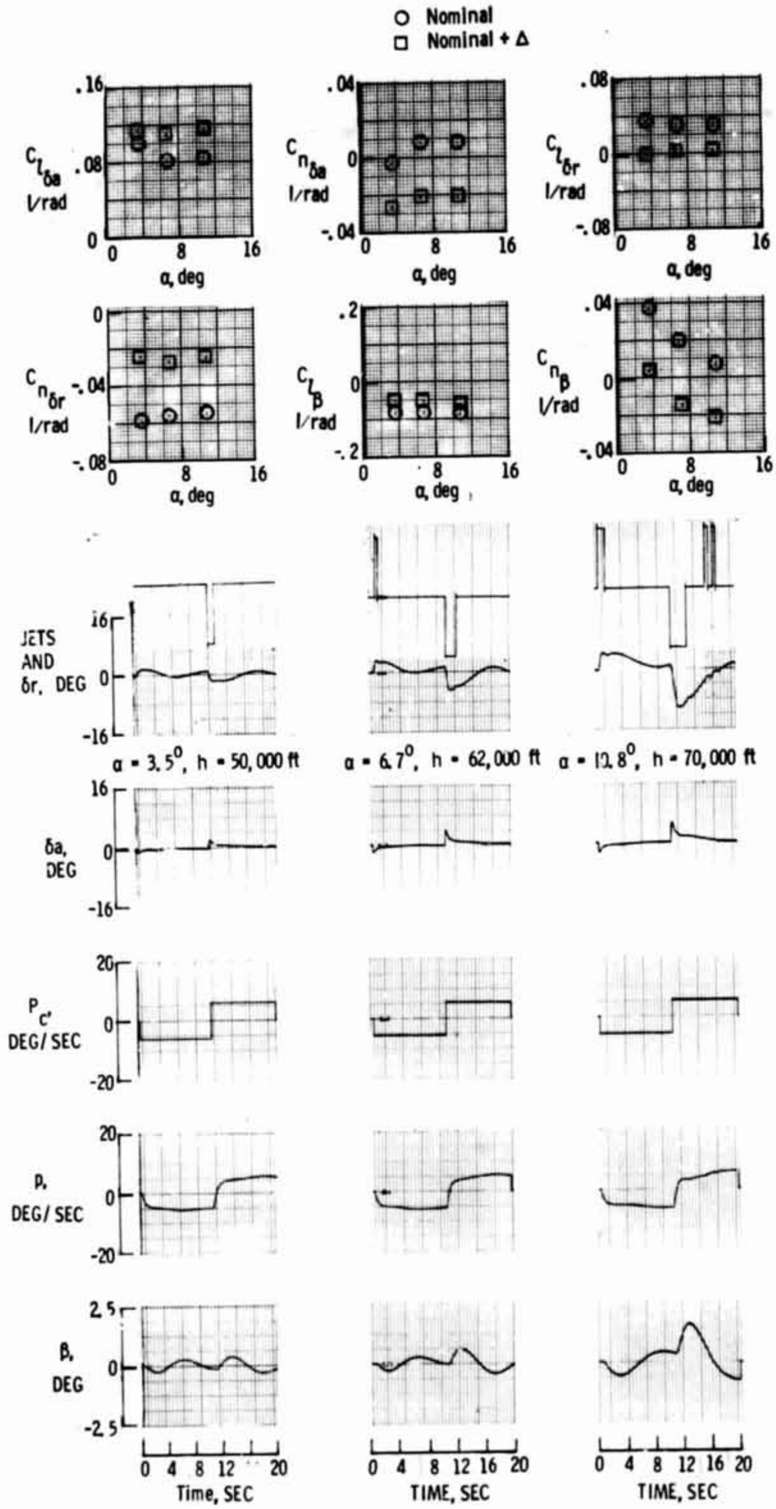

(a) Mach number 1.5

Figure 11.- The effects of variations in the sideslip, aileron, and rudder rolling and yawing moments.

ORIGINAL PAGE IS OF POOR QUALITY

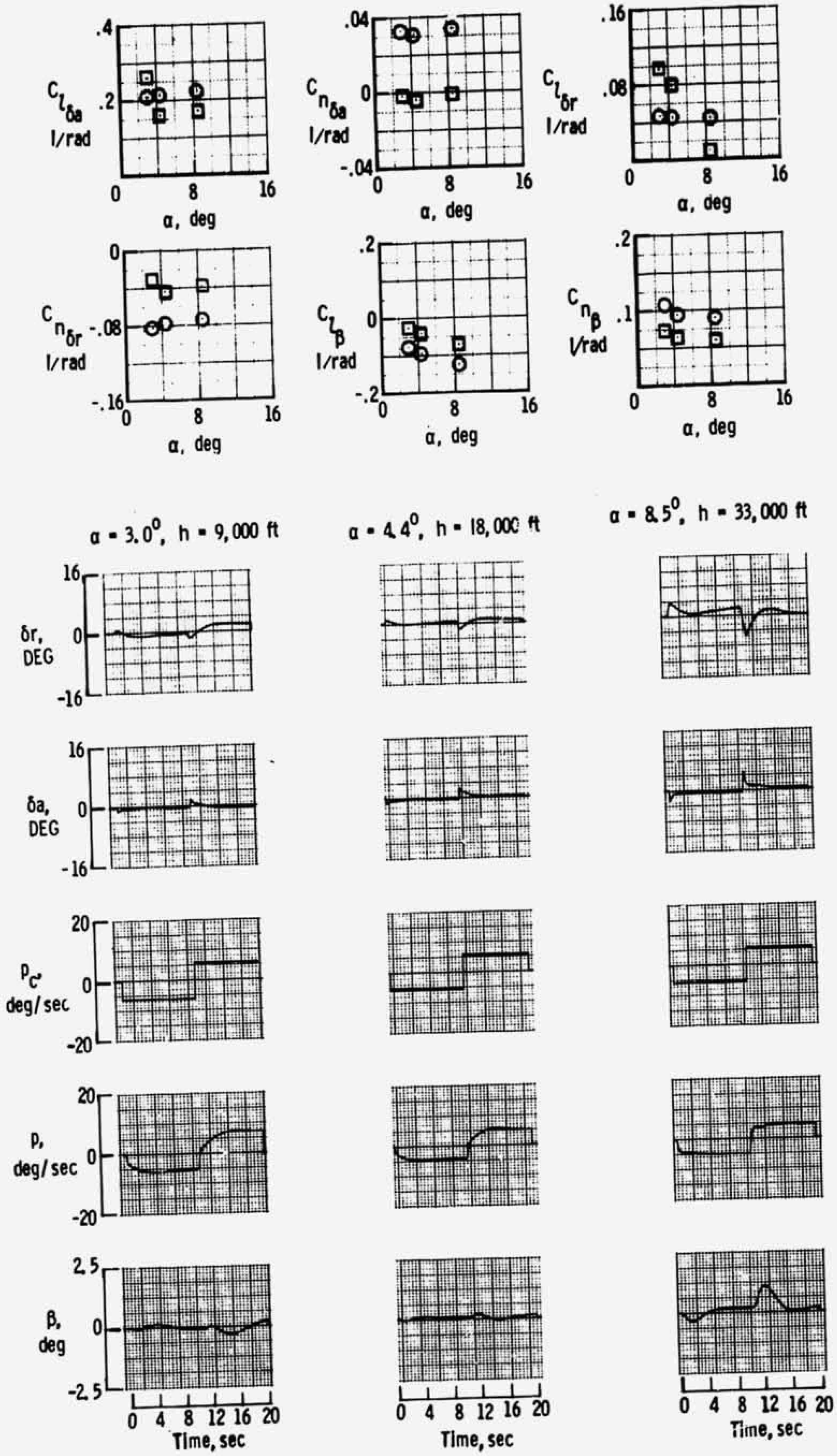

(b) Mach number .6

Figure 11.- Concluded.

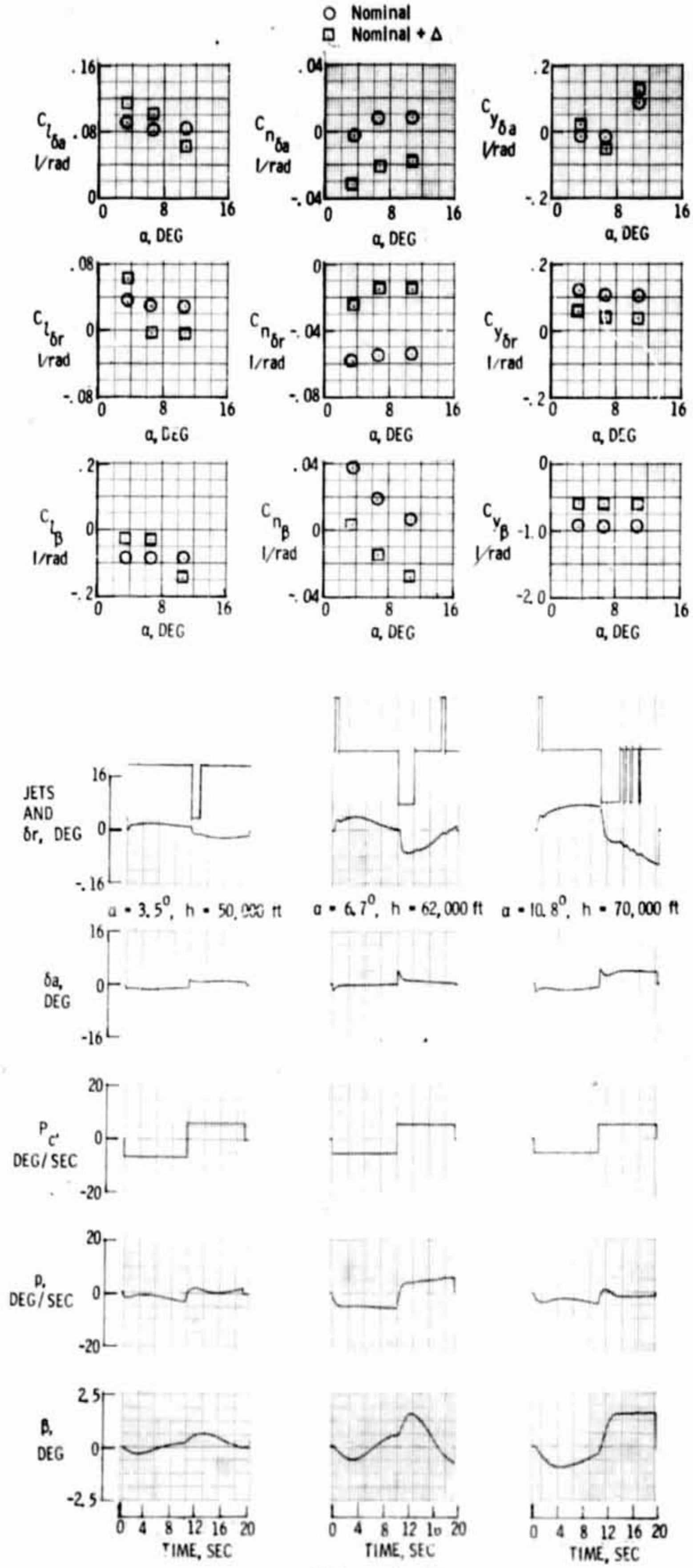

(a) Mach number 1.5

Figure 12.- The effects of variations in the sideslip, aileron, and rudder derivatives.

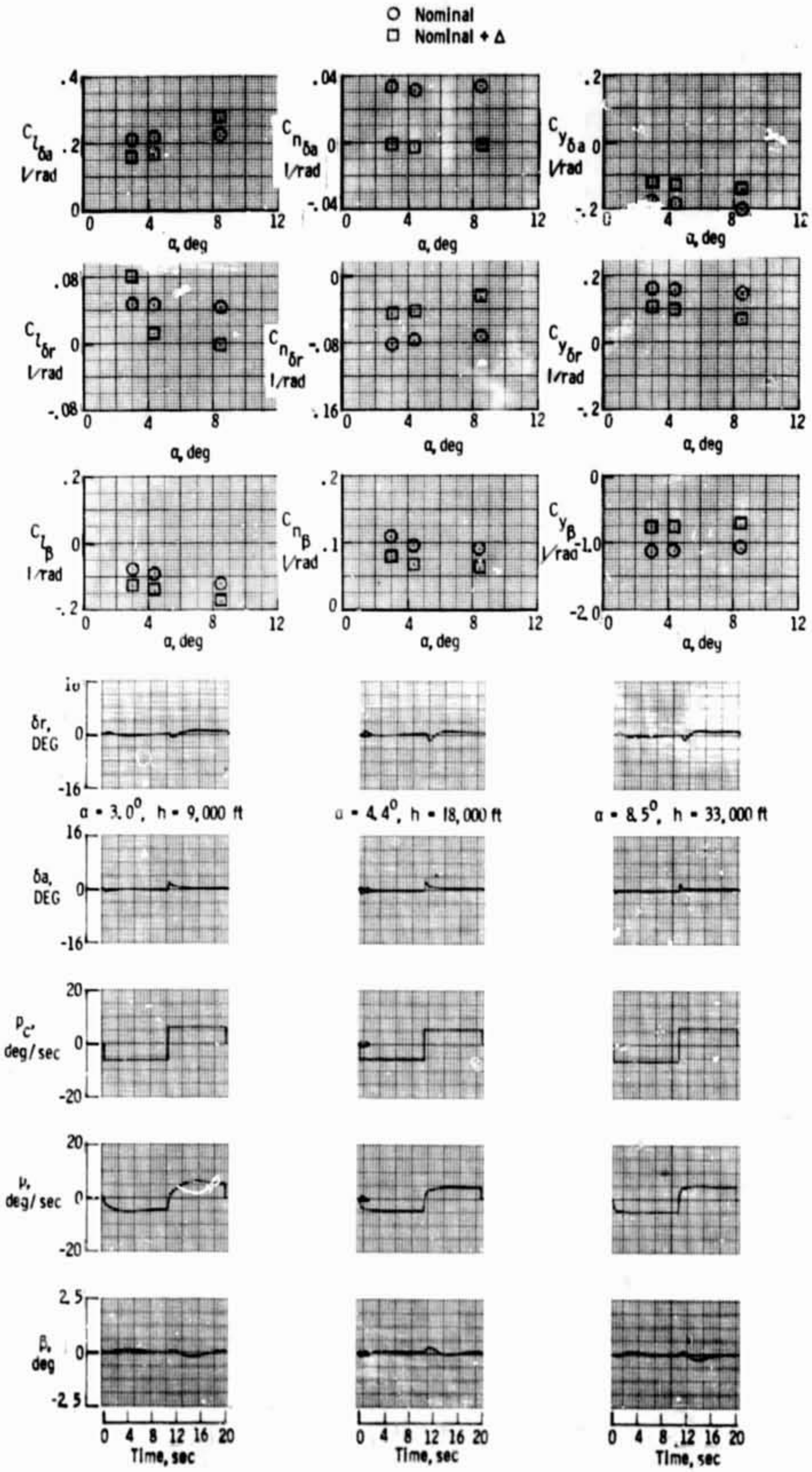

(b) Mach number .6

Figure 12.- Continued.

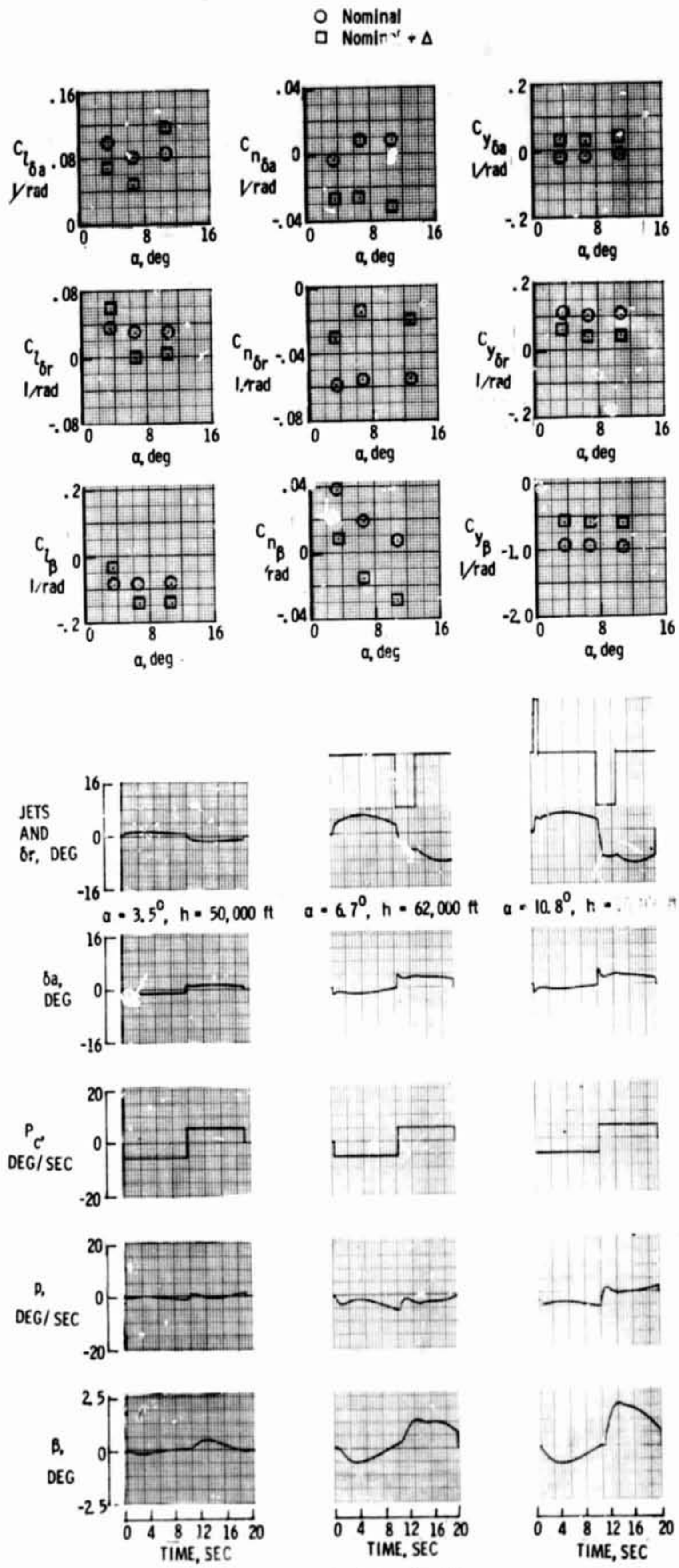

(c) Mach number 1.5

Figure 12.- Concluded.